bioRxiv preprint doi: https://doi.org/10.64898/2026.02.22.707324; this version posted February 23, 2026. The copyright holder for this preprint (which was not certified by peer review) is the author/funder, who has granted bioRxiv a license to display the preprint in perpetuity. It is made available under a CC-BY 4.0 International license.

International Journal of Cancer

WILEY

ORIGINAL ARTICLE OPEN ACCESS

Global dissemination of FC-ϵ RI and p53 signalling perturbation contribute to Dasatinib resistance in Pancreatic Cancer Cell-lines

AKM Azad[1] | Muhammad J. A. Shiddiky[2] | Mohammad Ali Moni[3]

[1]Department of Mathematics & Statistics,Faculty of Science, Imam Mohammad Ibn Saud Islamic University, Riyadh 13318, Saudi Arabia | [2]Rural Health Research Institute, Charles Sturt University, Orange NSW 2800, Australia | [3]Artificial Intelligence and Cyber Futures Institute, Charles Sturt University, Bathurst NSW 2795, Australia |

Correspondence: Mohammad Ali Moni (mmoni@csu.edu.au)

Received: **Revised:** **Accepted:**

Keywords: Pancreatic Cancer | Dastatinib | Acquired resistance | Cancer Cell-line | Biomarker discovery | Pathway Cross-talk Analysis | SPIA

ABSTRACT

Acquired Dasatinib Resistance (ADR) hinders efficacious treatment of Pancreatic Cancer (PC), often mediated by dynamic signalling reprogramming due to prolonged drug intake. With a novel signalling cross-talk network modelling, this study analyses transcriptomics data of dasatinib-resistant and dasatinib-sensitive pancreatic cancer cell lines and prioritizes key signalling molecules via systemic coordination of their magnitude of dysregulation and the degree of signalling cross-talk among enriched pathways. Results found the *p53* and *FC-ϵ RI signalling* pathways demonstrating significant perturbation enrichment, complementarily orchestrating a total of 87% of the global perturbation map in dasatinib resistance. Further statistical characterization of the cross-talk network identified 10 key resistant biomarkers, including *THBS1, CDKN1A*, and *BCL2L1* within *p53 signalling*, and *RAC2* and *MAPK13* within *FC epsilon RI signalling*. Validation with TCGA transcriptomics, CPTAC relative proteomics, and StringDB protein-protein interaction data for their potential prognostics revealed *BCL2L1* as pivotal for global perturbation dissemination and, thereby, a novel therapeutic target.

1 | Introduction

Pancreatic cancer (PC) is one of the most fatal cancers among all others due to its high mortality rate and poor early diagnosis [1]. Despite comprehensive treatment with chemo- and radiotherapy and complete tumour resection, a 5-year survival rate is only 13% [1]. Some chemotherapeutic agents, such as nab-Paclitaxel, gemcitabine, folfirinox, etc., have been used in clinical practices, but increased toxicity and severe-risk imposition upon highly metastatic patients render poor survival outcomes in PC patients [2].

Dasatinib, a multi-kinase inhibitor of Src family kinases commonly used to treat blood and bone marrow cancers, has also been approved by the Food and Drug Administration (FDA) for PC treatment [3] since Src inhibitors have the potential to reduce cell proliferation and induce cell cycle arrest in PC cells [4]. In pancreatic ductal adenocarcinoma (PDAC) cell lines (Panc-1 and Colo-357), dasatinib effectively blocks tumour stem cell generation via suppressing the expression of transforming growth factor-beta (TGF-β) target genes that are related to epithelial-mesenchymal transition and invasion [5].

Acquired resistance to targeted therapies emerges during the treatment of many cancers, including PC [6, 7], where the adaptive tumour microenvironment and epigenetic remodelling play crucial roles. In murine PDAC cells, aberrant methylation patterns were observed in multiple genomic sites of regulatory elements under increasing MEK_i treatment (MAPK pathway inhibitor), suggesting the epigenetic remodelling along with a single clonal expansion is responsible for its resistance [6]. Moreover, perturbation in signalling pathways leads to alternate activation of the compensatory signalling network [8, 9]. This phenotypic plasticity facilitates cancer cells to evade apoptosis, sustain

bioRxiv preprint doi: https://doi.org/10.64898/2026.02.22.707324; this version posted February 23, 2026. The copyright holder for this preprint (which was not certified by peer review) is the author/funder, who has granted bioRxiv a license to display the preprint in perpetuity. It is made available under a CC-BY 4.0 International license.

growth, and ultimately thrive in the presence of targeted therapy [8, 9].

Precise mechanisms underpinning acquired resistance (AR) to a drug require highly contextual analysis of relevant omics data. Therefore, we hypothesized that novel biomarkers contributing to Acquired Dasatinib Resistance (ADR) could be identified by seeking answers to the following research questions: 1) *which signalling proteins/genes/molecules are dysregulated in dasatinib-resistant vs dasatinib-sensitive cell lines?*, 2) *are their orchestrated activities involving the pathways (enriched with dysregulated entities) via signalling cross-talk?*, 3) *any particular signalling protein/gene/molecule that is driving the whole signalling perturbation?*. This study presents a comprehensive perturbation map of dasatinib resistance by leveraging high-throughput transcriptomic profiling of pancreatic cancer cell-line models. Initial screening of ADR biomarkers and their functional footprints is done via differential expression analysis, followed by their functional enrichment and signalling pathway impact analyses. Moreover, our approach identifies a novel map of highly aberrant perturbation drivers by employing a novel network-based modelling of signalling cross-talk networks. This has the potential to uncover key hubs and bottlenecks that drive resistance by disseminating the perturbation globally. The findings provide valuable insights into the molecular underpinnings of dasatinib resistance and establish a framework for the rational design of next-generation combination therapies for pancreatic cancer.

2 | Materials & Methods

Overall schematic diagram of our analysis workflow is shown in Figure 1.

Data Collection & Pre-processing

Gene expression data for Dasatinib-sensitive cell lines (Panc0504, Panc0403, Panc1005) and Dasatinib-resistant cell lines (MiaPaCa2, Panc1, SU8686) are collected from Gene Expression Omnibus (GEO) repositories with the accession number GSE59357. This dataset used three biological replicates to extract total RNA using complementary DNA microarray technology with the Illumina Human HT-12 v4 BeadChip (GPL10558). Two datasets (i.e., resistant and sensitive) were constructed via log2-transformation and quantile-normalization before further analyses were conducted.

Differential expression analysis

To identify a list of differential biomarkers, linear models were employed to resistant-vs-sensitive contrast matrices with empirical Bayes function and vooma transformation. Statistically significant differential expression changes were selected based on two thresholds: 1) $abs(log2FC) \geq 1.0$ (log2 fold change) and 2) FDR-adjusted $P.value \leq 0.05$.

Gene signature analysis

To observe the predominance of known gene signatures (as a predefined list of genes) in identified differentially expressed genes (Resistant-vs-Sensitive conditions), the GSEA (Gene Set Enrichment Analysis) was performed. It was hypothesized that Pancreatic cancer-related known gene signatures will be highly prevalent with differentially expressed genes in dastatinib resistance. The *gseDO* function from *DOSE* R package was used for this analysis, where the parameter values that were considered are: *nPerm=1000* (permutation iteration), *minGSSize=10* (minimal size of each geneSet), *maxGSSize=500* (maximum size of each geneSet), *pvalueCutoff=0.05*, and *pAdjustMethod="BH"* (benjamini-hochberg).

Functional pathway over-representation analysis

Enrichment of differentially expressed genes with known signalling pathways indicates strong relevance of their functional coherence. Therefore, a set of 48 signalling pathways from the KEGG (Kyoto Encyclopedia of Genes and Genomes) database [10] were collected for this purpose. To identify which signalling pathways are highly enriched with identified DEGs, a *Hypergeometric test*-based over-representation analysis is conducted using $phyper$ function (with $lower.tail = FALSE$) from *stats* R package with all the genes within the study as the background geneset. Statistically significant signalling pathways are defined with the enrichment $P.value \leq 0.05$ from the Hypergeometric test using the Equation **??**. The geneRatio values of each enriched pathway were computed by determining the ratio between the number of enriched DEGs and the size of the corresponding pathway.

$$P(X \geq x) = 1 - P(X \leq x-1) = 1 - \sum_{i=0}^{x-1} \frac{\binom{M}{i}\binom{N-M}{n-i}}{\binom{N}{n}} \quad (1)$$

where N = the total number of genes in the background gene list, M = genes in the Pathway, n = the number of DEGs used for this analysis, and the observed number x = the number of DEGs found within the given pathway. Here, the generated $P.value$ is a right-tail probability, i.e., $Pr(X \geq x)$, which determines the chance of having a larger number of overlaps than x. Hence, a smaller $P.value$ would indicate that the observed number of DEGs in the pathway is significantly higher than expected by chance, suggesting enrichment of the pathway with DEGs.

Cross-talk identification among enriched signalling pathways

An inter-pathway cross-talk network was constructed to examine systemic interactions among enriched signalling pathways via shared genes. Let $G := (V, G)$ be a signalling cross-talk network model, where V is the set of nodes representing either DEGs or pathways and E is the set of edges denoting the gene-pathway relationships obtained from signalling transduction pathways from KEGG database. Network construction was performed using the *igraph* R package. Cross-talking DEGs were defined as those connecting at least two pathways. Next, to identify perturbed and cross-talking DEGs, the network was filtered to retain only significant nodes (DEGs with $abs(log_2FC) \geq 2$) and pruned to exclude low-degree nodes (degree = 1). Node degree distribution was computed to observe the scale-free properties of the network. Central hubs, namely the *resistant biomarkers* were identified as nodes with high connectivity (the number of pathways cross-talking via it) and dysregulation ($abs(log_2FC)$). Pearson's correlation was

bioRxiv preprint doi: https://doi.org/10.64898/2026.02.22.707324; this version posted February 23, 2026. The copyright holder for this preprint (which was not certified by peer review) is the author/funder, who has granted bioRxiv a license to display the preprint in perpetuity. It is made available under a CC-BY 4.0 International license.

measured to quantify correlation between degree of the *resistant biomarkers* and their log_2FC. A *two-sided* and *two-sample Kolmogorov-Smirnov test* was conducted (using *ks.test* function from *base* R package) to test if the magnitude of differential expression of *resistant biomarkers* (i.e., cross-talking hubs) and its counterparts are drawn from the same distribution. The biological significance of hubs was assessed through literature mining and experimental evidence.

Signalling Pathway Impact Analysis

Over-representation-based enrichment analysis is a topology-unaware approach, which may lack mechanistic consideration. Therefore, the Signaling Pathway Impact Analysis (SPIA) was performed to quantify pathway perturbations integrating both over-representation of DEGs and pathway topology-driven signalling perturbation. It is hypothesized that the pathway perturbation through constituent signalling proteins depends both on their differential expressions and the perturbation activities of their upstream signalling proteins [11]. SPIA computes two probabilities: (1) pN_{DE}, representing the over-representation of DEGs in a pathway using a hypergeometric test [see Equation **??**], and (2) $pPERT$, quantifying the pathway perturbation propagated by DEGs through associated signalling links (activation or repression). The null hypothesis for $pPERT$ is that the total net accumulated perturbation tA [Equation 2] of a particular pathway is more than that of the observed one by chance [Equation 3], where the T_A is total net accumulated perturbation score of a particular bootstrap iteration, where the number of DEGs remains the same as an observed case, but to topology and differential expression fold-changes both were randomized.

$$tA = \sum Acc(g_i) \tag{2}$$

$$pPERT = Pr(T_A \geq t_A | H_0) \tag{3}$$

where the $Acc(g_i)$ is the net perturbation of a gene, g_i, calculated by the following Equation: [Equation 4]

$$Acc(g_i) = PF(g_i) - \Delta E(g_i) \tag{4}$$

where, $\Delta E(g_i)$ is the normalized expression changes of the gene g_i in resistant-vs-sensitive condition. Next, the $PF(g_i)$ is the perturbation factor of the gene g_i, which is determined by the following Equation [Equation 5]:

$$PF(g_i) = \Delta E(g_i) + \sum_{j=1}^{k} \beta_{ij} \times \frac{PF(g_j)}{N_{ds}(g_i)} \tag{5}$$

where $N_{ds}(g_j)$ is the number of downstream genes of g_j, and β_{ij} is a coefficient indicating the type of signalling link, i.e., activation or inhibition.

Next, for each pathway perturbation significance, a global p-value, namely pG, is determined by combining $pNDE$ and $pPERT$ by the "normal inversion" technique by setting the *combine* parameter as '*norminv*' [Equation 6].

$$pG = c - c \cdot ln\, c \tag{6}$$

where $c = pNDE \cdot pPERT$. The global p-value pG, is further corrected using both FDR and Bonferroni correction methods, termed as $pGFDR$ and $pGFWER$, respectively.

Visual interpretation of Pathway perturbation using PathView

To understand the perturbation effects of DEGs in a given enriched pathway, the *pathview* function from the *PathView* R package is used. PathView is a Bioconductor-hosted pathway analysis toolset which facilitates the seamless integration of differential expression results (user-supplied) and overlays the dysregulation information on the known pathway annotations. It automatically downloads the annotated genes, molecules and topology (inter-connections), parses it and renders the overlaid differential expression information.

Validation with Existing knowledge

Biomarkers are evaluated with multiple information sources - protein-protein association information from StringDB [12]. Evidence of potential prognostic values from gene expression changes from TCGA mRNA expression changes in Human Protein Atlas database [13]. StringDB web portal facilitates queries with multiple genes of a chosen species to output an induced sub-network with potential protein-protein interactions among them, defined by various sources of evidence, e.g., known interactions (database curated and experimentally verified), predicted (gene neighbourhood, gene fusions, and gene co-occurrence), text-mining, co-expression, and protein homology [12]. It also offers a set of network statistics regarding the output, including node and edge counts, average node counts, average local clustering coefficient (LCC), and statistical significance of the induced sub-network against the background (by randomizing the gene sets with the same size and degree distributions). Moreover, to facilitate further clustering, more nodes with their incident interactions from the whole PPI network (involving other genes in the whole genome) are augmented. For clustering the stochastic flow-based MCL (Markov Clustering) algorithm is employed with the inflation parameter thresholding. For reinforcement of the biological relevance of identified resistant biomarkers, further enrichment was conducted using GO terms (biological process), Reactome pathways, WikiPathways, Subcellular localizations information, and their Pubmed queries.

The Human Protein Atlas database has the gene expression from TCGA (The Cancer Genome Atlas) and protein expression from CPTAC (Clinical Proteomic Tumor Analysis Consortium) repositories for pancreatic adenocarcinoma (PAAD). Preprocessed transcriptomics (nRPX) data of Pancreatic cancer from 176 patients (84 alive and 92 deceased) with various stages (I, II, III, and IV) is observed for each biomarker in this study from the HPA database. TCGA RNA expression data from the HPA database were obtained for each of those resistant biomarkers. Using a "quartile"-based dichotomized of each gene expression (i.e., High or Low expression), survival analysis is performed using *survminer* R package. Tandem mass tag (TMT) mass spectrometry-based CPTAC proteomics data from 145 tumours and 90 normal was preprocessed, and relative proteomics expression was reported [13]. Relative protein expression of biomarkers genes from CPTAC data in Tumor-vs-Normal conditions were compared using *Wilcoxon test* to observe their differential abundance using *ggbetweenstats* R function (*ggstatsplot* R package [14]).

bioRxiv preprint doi: https://doi.org/10.64898/2026.02.22.707324; this version posted February 23, 2026. The copyright holder for this preprint (which was not certified by peer review) is the author/funder, who has granted bioRxiv a license to display the preprint in perpetuity. It is made available under a CC-BY 4.0 International license.

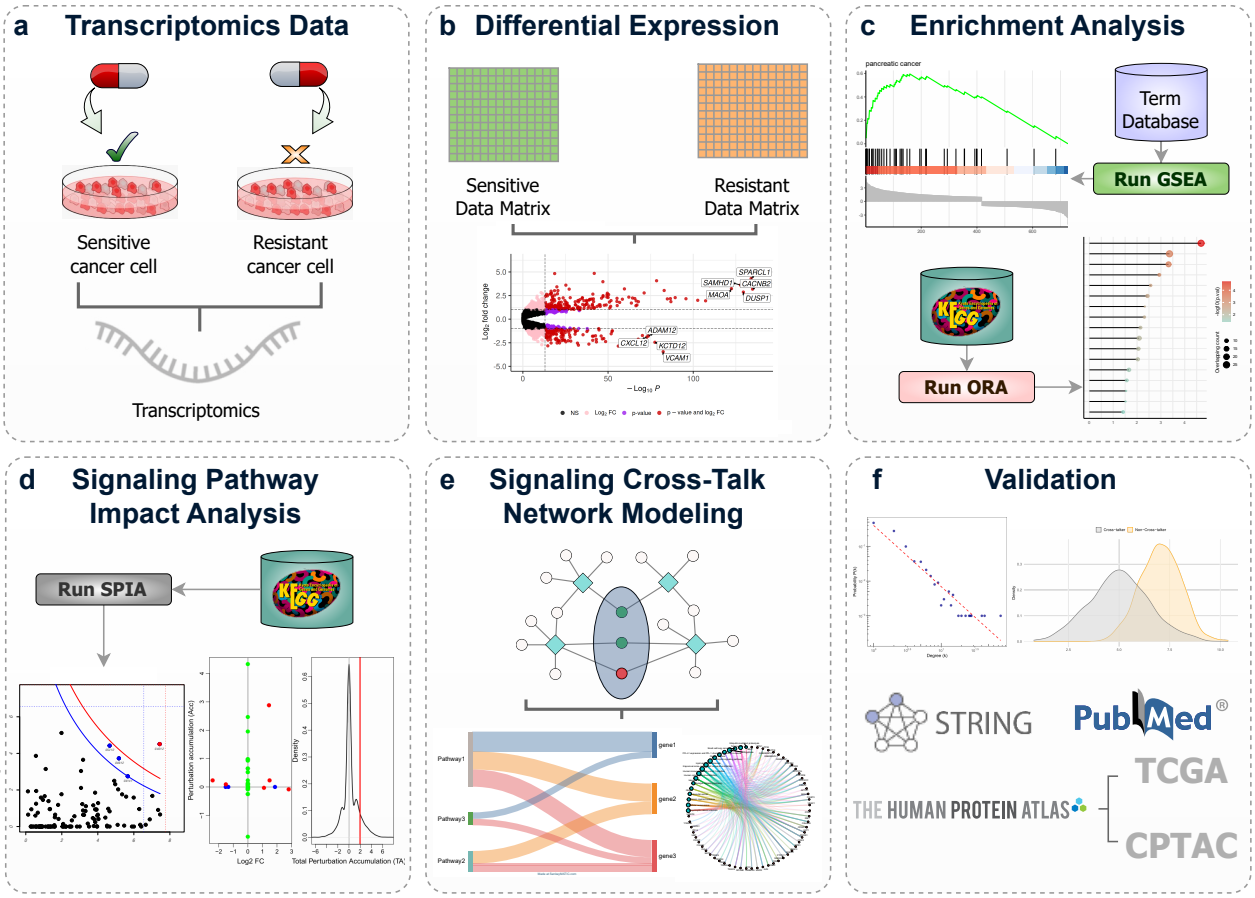


FIGURE 1 | Overall schematic diagram of our proposed workflow in identifying biomarkers of Acquired Dasatinib Resistance (ADR).

TABLE 1 | Top 20 up-regulated and down-regulated DEGs in Acquired Dasatinib resistance

	Gene.symbol	adj.P.Val	P.Value	t	B	logFC
Up-regulated	S100P	0.016	4.32E-04	4.217	0.054	5.151
	TACSTD2	0.015	3.57E-04	4.299	0.288	4.920
	LCN2	0.022	7.95E-04	3.955	-0.439	4.282
	KRT7	0.009	1.04E-04	4.832	1.411	4.275
	MSLN	0.012	2.33E-04	4.482	0.676	4.131
	GPX2	0.005	3.05E-05	5.371	2.559	4.126
	GDF15	0.012	2.31E-04	4.487	0.685	4.103
	CEACAM6	0.012	2.42E-04	4.466	0.611	4.043
	LAD1	0.007	5.77E-05	5.091	1.948	3.890
	MAL2	0.036	2.31E-03	3.496	-1.412	3.849
Down-regulated	JAM3	0.015	3.62E-04	-4.294	0.240	-3.179
	PRRX2	0.044	3.33E-03	-3.336	-1.834	-3.186
	SCG2	0.010	1.53E-04	-4.665	1.046	-3.251
	IRX3	0.005	3.12E-05	-5.363	2.505	-3.368
	COL5A2	0.046	3.80E-03	-3.278	-1.951	-3.381
	TM4SF18	0.011	1.64E-04	-4.636	1.001	-3.450
	TUBB2B	0.016	4.41E-04	-4.208	0.098	-3.563
	SRGN	0.025	1.11E-03	-3.812	-0.745	-3.639
	CBS	0.013	2.64E-04	-4.429	0.561	-3.645
	VIM	0.004	2.35E-05	-5.488	2.765	-5.121

bioRxiv preprint doi: https://doi.org/10.64898/2026.02.22.707324; this version posted February 23, 2026. The copyright holder for this preprint (which was not certified by peer review) is the author/funder, who has granted bioRxiv a license to display the preprint in perpetuity. It is made available under a CC-BY 4.0 International license.

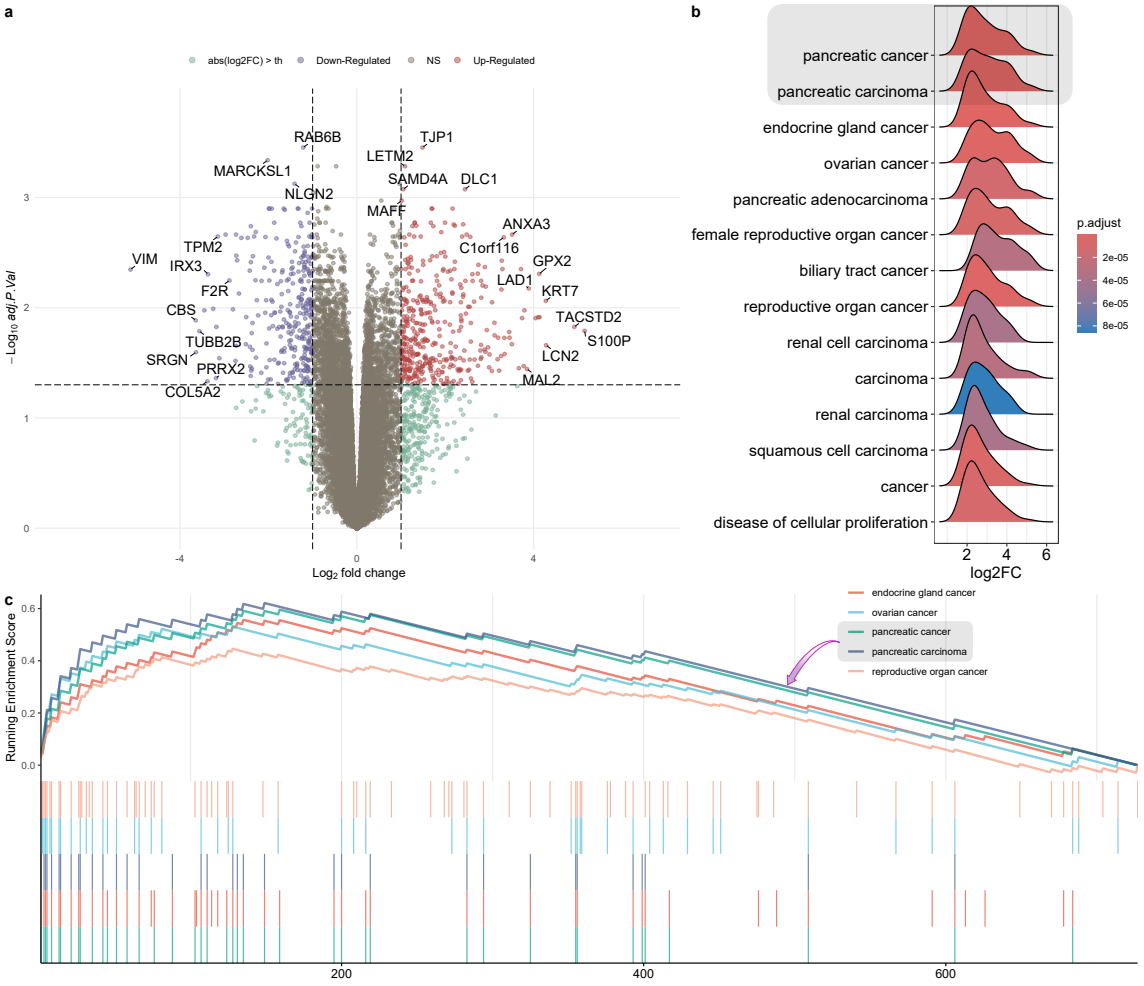


FIGURE 2 | **Differential Gene Expression Analysis**. **(a)** Volcano plot shows genes are differently expressed in acquired Dasatinib resistance-vs-sensitive conditions. **(b)** Geneset Enrichment analysis (GSEA) of 727 selected DEGs ($abs(log_2FC) \geq 1.0$ and FDR-adjusted $P.value < 0.05$), where most of the top enriched terms were pancreatic cancer-related, revealing the biological relevance of such differential expression in resistance-vs-sensitive conditions. **(c)** The distributions of running enrichment scores with pre-ranked gene list (727 DEGs) demonstrate that upregulation of pancreatic cancer as the gene-hits are clustered toward positive ranking metric, which indicates gene upregulations.

TABLE 2 | DEG-enriched KEGG Signalling pathways. Pathways are ordered based on overlapping GeneRatio (proportion of pathway genes that are enriched in a given pathway)

Description	Count	GeneRatio	pvalue	p.adjust
p53 signaling	8	0.107	0.001	0.013
Fc epsilon RI signaling	7	0.101	0.003	0.024
VEGF signaling	6	0.100	0.005	0.027
PPAR signaling	7	0.092	0.005	0.027
NF-kappa B signaling	9	0.086	0.004	0.027
MAPK signaling	25	0.083	0.000	0.001
Phosphatidylinositol signaling system	8	0.082	0.007	0.034
Rap1 signaling	17	0.080	0.000	0.007
TNF signaling	9	0.076	0.009	0.034
Neurotrophin signaling	9	0.075	0.009	0.034
B cell receptor signaling	6	0.071	0.029	0.084
ErbB signaling	6	0.070	0.030	0.084
PI3K-Akt signaling	25	0.069	0.000	0.007
Wnt signaling	12	0.069	0.008	0.034
Sphingolipid signaling	8	0.066	0.027	0.084
Hippo signaling	10	0.064	0.022	0.074
Relaxin signaling	8	0.062	0.038	0.099

bioRxiv preprint doi: https://doi.org/10.64898/2026.02.22.707324; this version posted February 23, 2026. The copyright holder for this preprint (which was not certified by peer review) is the author/funder, who has granted bioRxiv a license to display the preprint in perpetuity. It is made available under a CC-BY 4.0 International license.

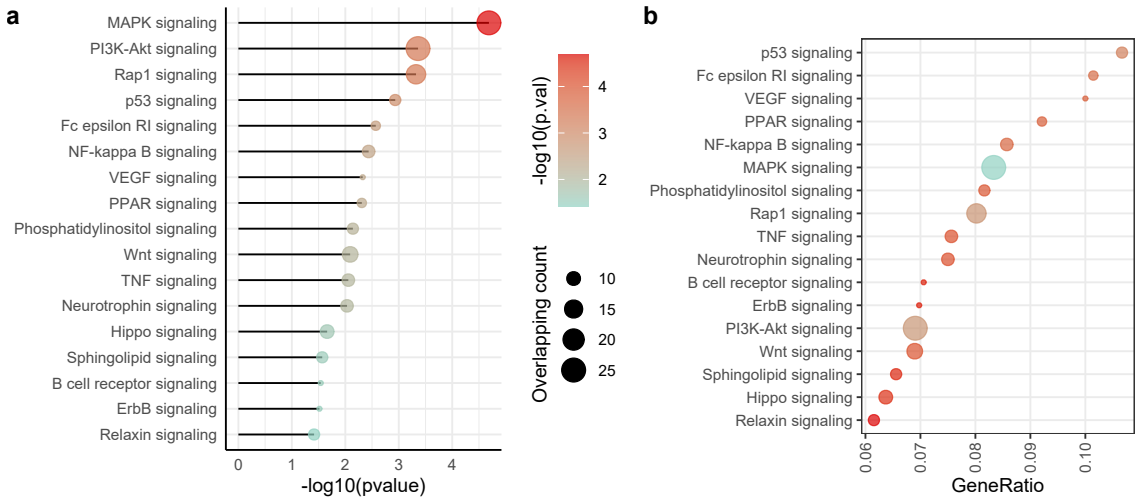


FIGURE 3 | **Functional enrichment analysis of DEGs with known signalling pathways from KEGG**. DEGs (adjusted p-value < 0.01) were subjected to the signalling pathway (KEGG) enrichment analysis using a Hypergeometric test - revealing significantly ($P.value \leq 0.05$) enriched signalling pathways with high enrichment geneRatio values, including p53, Fc epsilon RI, VEGF, PPAR, and NF-kappa B signalling pathways.

TABLE 3 | p53 signalling pathways cross-talking with other signalling pathways via highly up-regulated shared genes.

Pathway1	Pathway2	Shared Gene	log2FC	adj.P.Val
p53 signaling	ErbB signaling	CDKN1A	2.738	0.034
	Hippo signaling	CCND1	1.111	0.013
	MAPK signaling	GADD45A	1.280	0.011
	NF-kappa B signaling	PPP1R13L	1.336	0.018
	NF-kappa B signaling	GADD45A	1.280	0.011
	NF-kappa B signaling	BCL2L1	1.993	0.002
	PI3K-Akt signaling	THBS1	3.336	0.019
	PI3K-Akt signaling	CCND1	1.111	0.013
	PI3K-Akt signaling	CDKN1A	2.738	0.034
	PI3K-Akt signaling	BCL2L1	1.993	0.002
	Rap1 signaling	THBS1	3.336	0.019
	Wnt signaling	CCND1	1.111	0.013

bioRxiv preprint doi: https://doi.org/10.64898/2026.02.22.707324; this version posted February 23, 2026. The copyright holder for this preprint (which was not certified by peer review) is the author/funder, who has granted bioRxiv a license to display the preprint in perpetuity. It is made available under a CC-BY 4.0 International license.

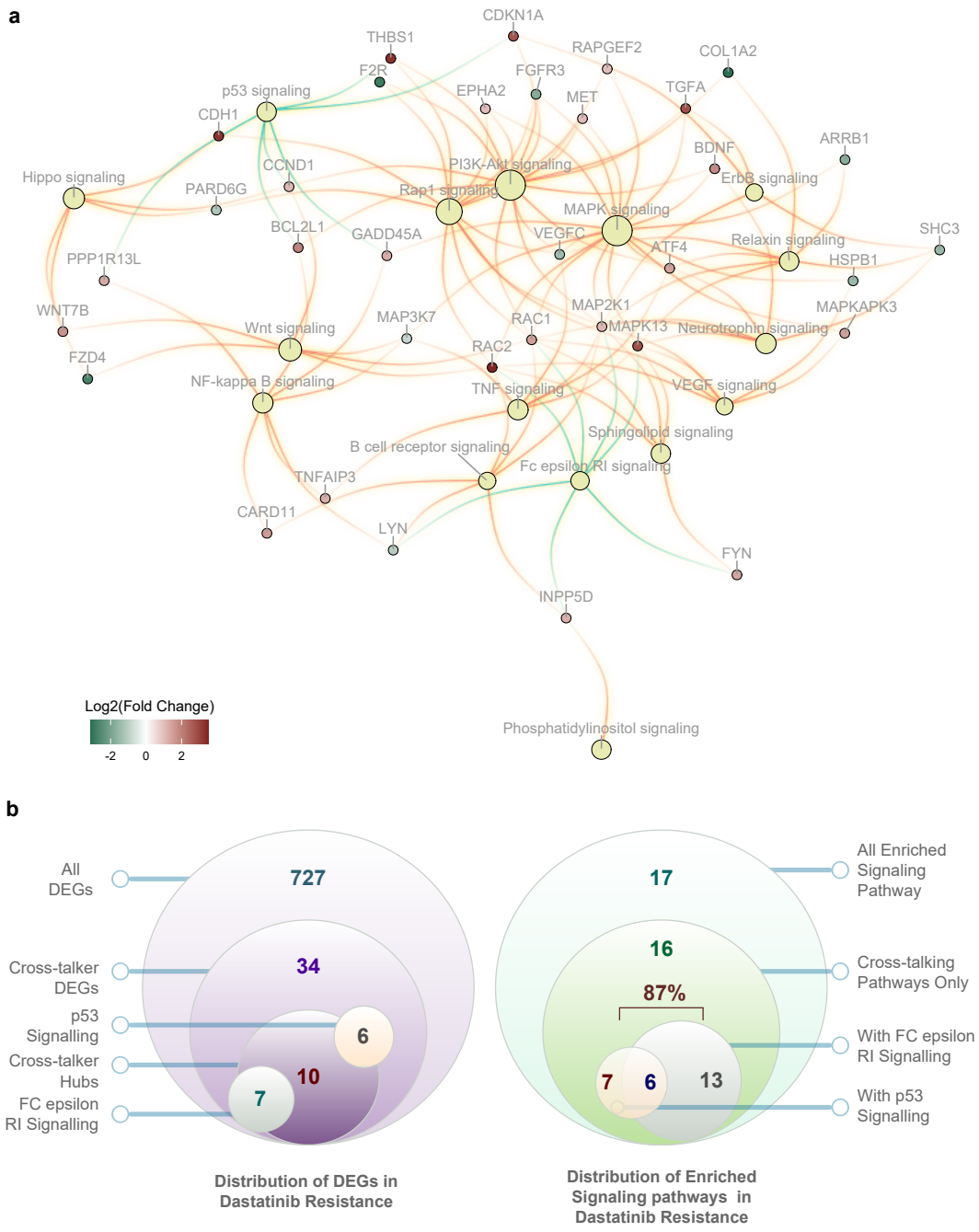


FIGURE 4 | **Signalling cross-talks among DEG-enriched KEGG signalling pathways. (a)** Enriched signalling pathways were found to be cross-talking among themselves involving highly over-expressed (e.g., SHC3, TGFA, THBS1, BDNF, BCL2L1, WNT7B, CCND1, and VEGFC) genes and under-expressed (e.g., PPP1R13L, RAC1, RAC2, CARD11, F2R, FYN, LYN, and FZD4) in Dasatinib-sensitive versus Dastatinib-resistant conditions. p53 and FC epsilon RI signalling pathways (green colour edges) - two of the most highly enriched pathways (based on geneRatio values) were highly complementary in coordinating these cross-talks as they shared no constituent genes between them. Note, each genes are also coloured in proportion to their differential expression level (i.e., log_2-scale) **(b)** Distribution of cross-talker DEGs and their enriched Signalling pathways, particularly in p53 and FC epsilon signalling pathways which combinedly cross-talks with 87% of all signalling pathways involved, indicating the dominance in driving global perturbation.

3 | Results

Dasatinib is a dual inhibitor of Abl/Src tyrosine kinases, normally used for treating Ph-positive leukaemia, but has shown competence in Pancreatic ductal adenocarcinoma (PDAC) in pre-clinical studies [15]. However, its efficacy in clinical settings wasn't promising, primarily due to the acquired resistance [16].

bioRxiv preprint doi: https://doi.org/10.64898/2026.02.22.707324; this version posted February 23, 2026. The copyright holder for this preprint (which was not certified by peer review) is the author/funder, who has granted bioRxiv a license to display the preprint in perpetuity. It is made available under a CC-BY 4.0 International license.

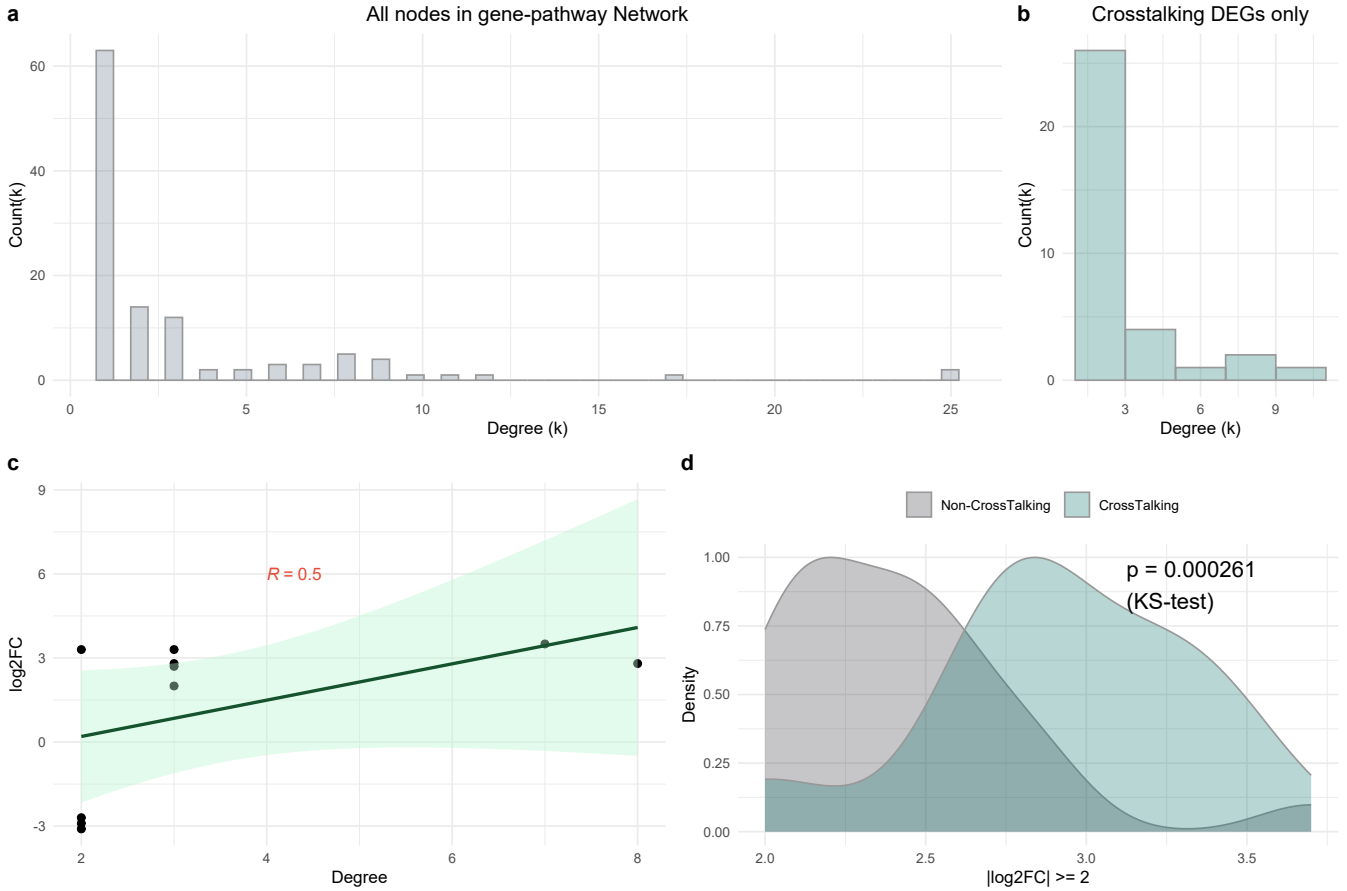


FIGURE 5 | Scale-Free topology of cross-talk network and the association of its cross-talking hubs with their differential expression in resistance conditions. **(a)** Gene-Pathway cross-talk network reveals the scale-free topology where only a few nodes have very large connectivity. **(b)** Similar scale-free pattern was observed when only cross-talking DEGs ($degree \geq 2$) were considered, **(c)** For the cross-talking DEGs ($degree \geq 2$) that have high differential expression ($log_2FC \geq 2$ or $log_2FC \leq -2$) (a total of 9 DEGs), a moderate correlation ($R = 0.51$) was observed between their degree of connectivity and degree of dysregulation. **(d)** Moreover, compared to the non-cross-talking DEGs, those 9 cross-talking DEGs demonstrated a statistically significant difference in the distribution of dysregulation when a filter of $abs(log_2FC) > 2$) was applied for all the DEGs in the network.

In this study, we have investigated the role of differential biomarkers in signalling perturbation in resistance-vs-sensitive cell lines and their impact on dasatinib resistance. We hypothesized that key signalling biomarkers and their network-based signalling impact analysis might reveal the putative mechanisms of acquired resistance to dasatinib in Pancreatic cancer cell lines.

Differential Expression Analysis and GSEA-based Initial Insights into Biological Relevance

We collected gene expression datasets of pancreatic cancer cell lines with Dastatinib-sensitive and Dastatinib-resistant conditions, which were further preprocessed using log2-transformation and quantile-normalization using *limma* R package. Then, we performed differential expression analysis in resistant-vs-sensitive using linear models with empirical Bayes with *vooma* using *limma* R package. After applying a combined threshold of $abs(log_2FC) \geq 1.0$ (log2 fold change) and FDR-adjusted $P.value \leq 0.05$, we have obtained a total of 727 differentially expressed genes (DEGs) [Supplementary table 1], among which 417 genes were up-regulated and 310 were down-regulated. Top 20 DEGs (based on log_2FC) are shown in Table 1, where VIM, CBS, SRGN, TUBB2B, and TM4SF18 are some highly downregulated DEGs, and S100P, TACSTD2, LCN2, KRT7, and MSLN are a few highly upregulated DEGs [Figure 2a]. To observe the biological relevance of the identified DEGs in acquired dasatinib resistance in pancreatic cancer, we have conducted a GSEA (Gene Set Enrichment Analysis) using *fgsea* with minimum and maximum size of each geneset 10 and 500, respectively. Highly enriched biological terms were selected based on a filter: Benjamini-Hochberg-adjusted adjusted $P.value < 0.0001$, yielding 14 terms. Among these, the most prominently enriched terms include: *"pancreatic cancer"* [normalized enrichment score (NES) = 3.03, FDR = 6.4×10^{-10}, 27 DEGs matches], *"pancreatic carcinoma"* [NES = 3.01, FDR = 1.7×10^{-8}, 22 DEGs matches] and *"pancreatic adenocarcinoma"* [NES = 2.75, FDR = 4.02×10^{-7}, 15 DEGs matches] [Figure 2b], where the visualization of distributions of running enrichment scores with pre-ranked gene list (727 DEGs) suggests that top terms are shown highly enriched with upregulated genes [Figure 2c]. These results suggest that significant DEGs are highly contextual towards pancreatic cancer metastasis and/or acquired resistance towards dasatinib drug in pancreatic cancer.

bioRxiv preprint doi: https://doi.org/10.64898/2026.02.22.707324; this version posted February 23, 2026. The copyright holder for this preprint (which was not certified by peer review) is the author/funder, who has granted bioRxiv a license to display the preprint in perpetuity. It is made available under a CC-BY 4.0 International license.

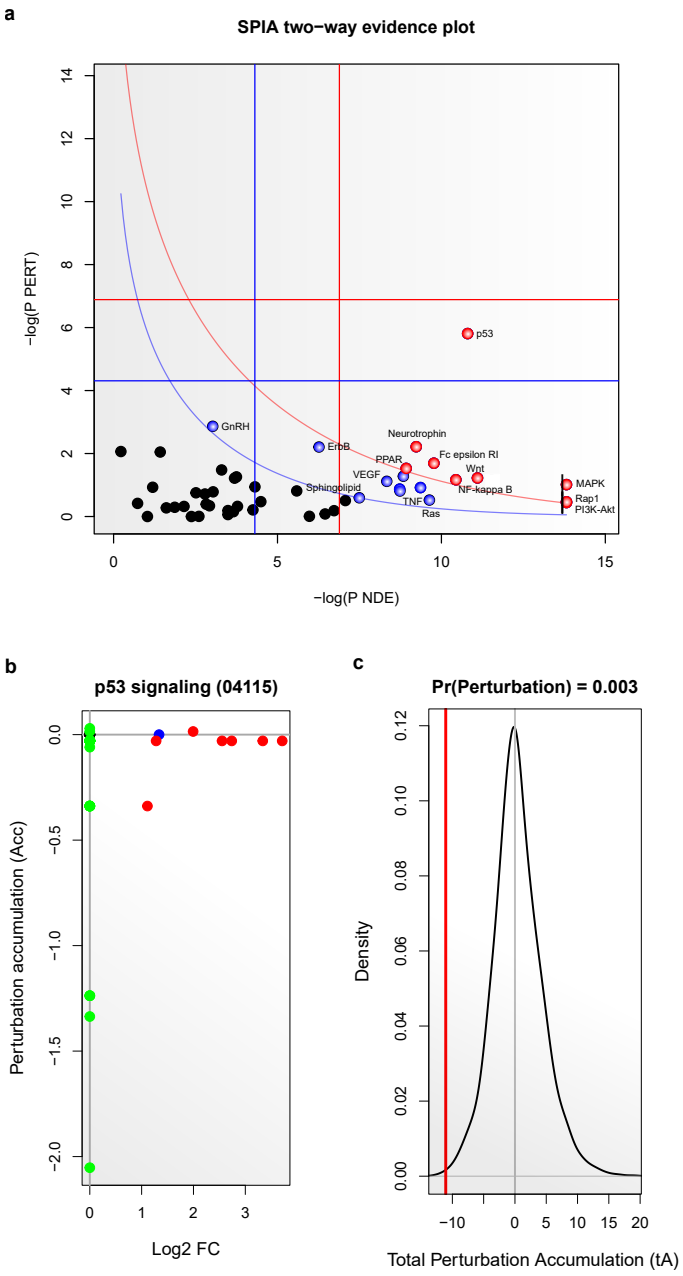


FIGURE 6 | Signaling Pathway Impact Analysis (SPIA) for using the DEGs (i.e., log fold changes) on 49 KEGG signalling pathways topologies. (a) By combining the over-representation probability (pNDE) with DEGs and topology-based Perturbation probability (pPERT), the two-way evidence plot reveals the ErbB, Estrogen, PI3K-Akt, and GnRH signalling pathways (red circles) as statistically significant (Bonferroni-corrected *P*-value < 0.05) that are also biologically relevant (i.e., contributing to the Dasatinib-resistance mechanisms). Including the above, the p53, Hippo, Neurotrophin, TNF, Thyroid hormone, and Sphingolipid signalling pathways were also found statistically significant (FDR-corrected *P*-value < 0.05). **(b)** Relationship of differential expression and pathway perturbation activity The Presence of potential drivers of the perturbation can be observed through either high perturbation score and/or significant expression changes. **(c)** Statistical significance of the negative total perturbation shows the potentially critical role of this pathway inhibition in dasatinib resistance mechanisms. **(d)** Pathview plots for the DEGs demonstrate their significant downstream effect contributing to dastatinib resistance mechanisms. These include downregulation of apoptosis (via CASP8), Increased inhibition of angiogenesis and metastasis, inhibition of IGF-I/mTOR pathway, etc.

Over-Representation Analysis of KEGG Signaling Pathways

To determine the signalling perturbation effects of the DEGs, we performed an over-representation-based pathway enrichment test (i.e., Hypergeometric test) against known 48 KEGG signalling pathways, where the whole list of genes in this cohort was considered as the background gene set. Using a threshold of enrichment $P.value \leq 0.05$ (from Hypergeometric test), we obtained 17 signalling pathways as significantly enriched with the DEGs [Fig 3a]. Among those, *p53*, *Fc epsilon RI, VEGF, PPAR, NF-κB*, and *MAPK* signalling pathways were highly enriched based on the enrichment gene ratio [Fig 3b], which is a proportion of pathway genes that are enriched in a given pathway [Table 2].

bioRxiv preprint doi: https://doi.org/10.64898/2026.02.22.707324; this version posted February 23, 2026. The copyright holder for this preprint (which was not certified by peer review) is the author/funder, who has granted bioRxiv a license to display the preprint in perpetuity. It is made available under a CC-BY 4.0 International license.

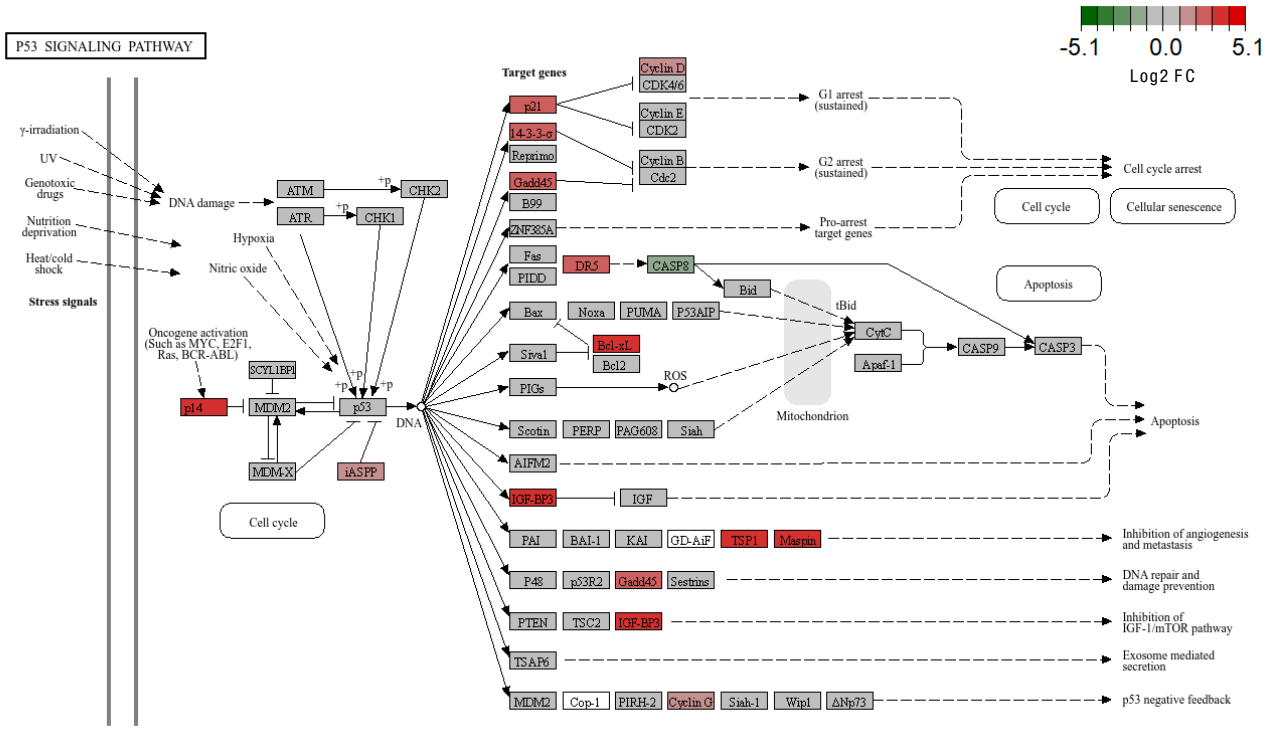


FIGURE 7 | p53 Signalling pathway Perturbation. Pathview plot for the DEGs demonstrates their significant downstream effect contributing to dastatinib resistance mechanisms. These include downregulation of apoptosis (via CASP8), Increased inhibition of angiogenesis and metastasis, inhibition of IGF-I/mTOR pathway, etc .

P53 and FC epsilon RI Signaling Cross-Talks are crucial in disseminating overall perturbation

Pathway enrichment tests reveal important functional footprints of differential biomarkers. However, it lacks the insights of detailed coordination among those enriched functional terms. Therefore, we performed a signalling cross-talk analysis among 17 top enriched KEGG signalling pathways, where the cross-talk between two pathways was identified via a shared component (gene/protein/molecule) that is a constituent of both [17, 8, 9, 18]. Figure 4a shows the network view of these signalling cross-talks, how the involved pathways are interconnected and share their perturbations. In this network, the nodes are either DEGs and their enriched signalling pathways, and the edges are the pathway-DEG memberships. Hence, any DEG that is shared between two pathways is considered to be a cross-talking bridge between those pathways. Note that this network is constructed in an ad-hoc manner, which doesn't necessarily indicate physical protein-protein interaction, and regarding the DEGs in this network, the ones that are not shared with at least two pathways are pruned out. Thus, we obtained 16 signalling pathway nodes and 34 DEG nodes in this network [Figure 4a]. Here, pathway node sizes are proportionate to the number of DEGs involved, and DEG node colours are proportionate to the degree of their log2 fold changes. We were particularly interested in observing the signalling pathways that were found to be highly enriched with higher geneRatio (see Table 2), as it highlights the pathways in a size-invariant manner. As *p53* and *FC epsilon RI signalling* pathways were shown higher geneRatio than others (post-filtration with enrichment $P.value < 0.05$), we investigated those two pathways further. Table 3 and Table 4 show *p53* and *FC epsilon RI signalling* pathways and their cross-talking pathways, respectively, via their shared DEGs and their corresponding log_2-fold changes and $adjusted\text{-}P.values$. It reveals that *p53 signalling* pathway was involved with a total of 6 DEGs (**CDKN1A, CCND1, GADD45A, PPP1R13L, BCL2L1**, and **THBS1**), involving 7 of 16 signalling pathways (43.8%) [Figure 4b]. Regarding *FC epsilon RI signalling* pathways, a total of 7 DEGs (**LYN, INPP5D, RAC1, RAC2, MAP2K1, MAPK13**, and **FYN**) are defined as cross-talks involving 13 of 16 signalling pathways (81.2%) [Figure 4b]. Interestingly, except the "*Hippo signalling*", 6 others that were found to be cross-talking with *p53 signalling* pathway were also found to be within 13 cross-talking pathways with *FC epsilon RI signalling*. This indicates that *p53* and *FC epsilon RI signalling* pathways combinedly cross-talk with 14 out of all 16 signalling pathways in this network, which is 87.5% [Figure 4b].

Scale-Free Topology Identifies Key Crosstalk Hubs Driving Resistance-Induced Dysregulation Cascade

Next, we investigated the biological relevance and analytical rigour of such gene-pathway cross-talk [see 3] by observing the potential existence of its scale-free topology. Therefore, we determined the degrees of all the network nodes and observed their frequency distribution. The results suggest that a few nodes (hubs) exhibit disproportionately high connectivity compared to the rest [Figure 5a], a hallmark of scale-free topology in biological

bioRxiv preprint doi: https://doi.org/10.64898/2026.02.22.707324; this version posted February 23, 2026. The copyright holder for this preprint (which was not certified by peer review) is the author/funder, who has granted bioRxiv a license to display the preprint in perpetuity. It is made available under a CC-BY 4.0 International license.

TABLE 4 | FC epsilon RI signalling pathways cross-talking with other signalling pathways via DEGs.

Pathway1	**Pathway2**	**Shared Gene**	**log2FC**	**adj.P.Val**
Fc epsilon RI signaling	B cell receptor signaling	LYN	-1.061	0.019
	B cell receptor signaling	INPP5D	1.266	0.015
	B cell receptor signaling	RAC1	1.491	0.038
	B cell receptor signaling	RAC2	3.506	0.021
	B cell receptor signaling	MAP2K1	1.106	0.019
	ErbB signaling	MAP2K1	1.106	0.019
	MAPK signaling	MAP2K1	1.106	0.019
	MAPK signaling	RAC1	1.491	0.038
	MAPK signaling	RAC2	3.506	0.021
	MAPK signaling	MAPK13	2.801	0.029
	NF-kappa B signaling	LYN	-1.061	0.019
	Neurotrophin signaling	RAC1	1.491	0.038
	Neurotrophin signaling	MAPK13	2.801	0.029
	Neurotrophin signaling	MAP2K1	1.106	0.019
	PI3K-Akt signaling	MAP2K1	1.106	0.019
	PI3K-Akt signaling	RAC1	1.491	0.038
	Phosphatidylinositol signaling	INPP5D	1.266	0.015
	Rap1 signaling	RAC1	1.491	0.038
	Rap1 signaling	RAC2	3.506	0.021
	Rap1 signaling	MAP2K1	1.106	0.019
	Rap1 signaling	MAPK13	2.801	0.029
	Relaxin signaling	MAPK13	2.801	0.029
	Relaxin signaling	MAP2K1	1.106	0.019
	Sphingolipid signaling	RAC1	1.491	0.038
	Sphingolipid signaling	RAC2	3.506	0.021
	Sphingolipid signaling	MAPK13	2.801	0.029
	Sphingolipid signaling	FYN	1.410	0.021
	Sphingolipid signaling	MAP2K1	1.106	0.019
	TNF signaling	MAPK13	2.801	0.029
	TNF signaling	MAP2K1	1.106	0.019
	VEGF signaling	RAC1	1.491	0.038
	VEGF signaling	RAC2	3.506	0.021
	VEGF signaling	MAPK13	2.801	0.029
	VEGF signaling	MAP2K1	1.106	0.019
	Wnt signaling	RAC1	1.491	0.038
	Wnt signaling	RAC2	3.506	0.021

TABLE 5 | 10 Cross-talking hubs as significant biomarkers in Dasatinib resistance

Biomarkers	Cross-talk degree	Differential fold change
COL1A2	2	-3.1
F2R	2	-2.9
FZD4	2	-2.7
BCL2L1	3	2
CDKN1A	3	2.7
TGFA	3	2.8
MAPK13	8	2.8
THBS1	3	3.3
CDH1	2	3.3
RAC2	7	3.5

TABLE 6 | SPIA (Signaling Pathway Impact Analysis) for DEGs to identify pathway perturbation activities. Results are shown only with the significantly perturbed pathways (pGFWER < 0.05) in a sorted manner based on the perturbation p-value, pPERT.

Pathway Name	pNDE	tA	pPERT	pG	pGFdr	pGFWER	Status
p53 signaling	2.0E-05	-11.056	0.003	6.4E-07	1.5E-05	3.1E-05	Inhibited
Neurotrophin signaling	9.8E-05	16.754	0.109	2.3E-04	2.2E-03	1.1E-02	Activated
Fc epsilon RI signaling	5.7E-05	14.815	0.184	3.8E-04	2.9E-03	1.8E-02	Activated
PPAR signaling	1.3E-04	1.974	0.217	8.7E-04	4.6E-03	4.2E-02	Activated
Wnt signaling	1.5E-05	7.124	0.294	4.3E-04	2.9E-03	2.1E-02	Activated
NF-kappa B signaling	2.9E-05	-7.492	0.311	7.1E-04	4.3E-03	3.4E-02	Inhibited
MAPK signaling	8.6E-12	8.033	0.363	2.8E-07	1.3E-05	1.3E-05	Activated
Rap1 signaling	2.6E-08	7.620	0.627	1.5E-04	1.8E-03	7.0E-03	Activated
PI3K-Akt signaling	4.4E-10	8.351	0.642	2.3E-05	3.6E-04	1.1E-03	Activated

bioRxiv preprint doi: https://doi.org/10.64898/2026.02.22.707324; this version posted February 23, 2026. The copyright holder for this preprint (which was not certified by peer review) is the author/funder, who has granted bioRxiv a license to display the preprint in perpetuity. It is made available under a CC-BY 4.0 International license.

TABLE 7 | Validation of resistant biomarkers with CPTAC Proteomics and TCGA transcriptomics in PAAD

		CPTAC Proteomics data			TCGA Transcriptomics
Gene	**Gene name**	**p-value**	**Adjusted p-value**	**logFC**	**P-value**
ENSG00000137801	THBS1	< 2.2E-16	1.90E-22	1.54446	0.24
ENSG00000164692	COL1A2	< 2.2E-16	3.94E-18	1.03198	0.23
ENSG00000156711	MAPK13	3.10E-13	3.76E-09	-0.426083	0.58
ENSG00000171552	**BCL2L1**	**6.10E-13**	**6.58E-09**	**0.897466**	2.2×10^{-04}
ENSG00000039068	CDH1	1.10E-11	6.98E-08	-0.403692	0.16
ENSG00000181104	F2R	8.50E-05	5.23E-01	0.812324	0.75
ENSG00000124762	CDKN1A	0.34	1.00E+00	0.139532	0.12
ENSG00000128340	RAC2	1.50E-04	1.00E+00	0.299814	0.14
ENSG00000163235	TGFA	–	–	–	9.2×10^{-04}
ENSG00000163235	FZD4	–	–	–	0.075

networks [19]. Moreover, we observed similar behaviour when we only selected DEG nodes (ignoring their associated pathway nodes) [Figure 5b].

Having the scale-free property within the network topology, it is also worth investigating the association of differential expression changes of DEGs in resistant conditions compared to sensitive conditions. This is crucial for prioritizing hub cross-talks (i.e., DEGs) with high-degree centralities that exhibit significant differential expression as those may not only be key regulators of resistance-causing perturbations but also be targeted by therapeutics. In that regard, we investigated the cross-talking DEGs (i.e., $degree \geq 2$, shared by at least two pathways) that have higher differential expression in resistant-vs-sensitive cell lines (i.e., $log_2FC \geq 2$ or $log_2FC \leq -2$) than others. This selection strategy yielded a total of 10 cross-talking DEGs, which revealed a moderate correlation ($R = 0.5$) between the node degrees of cross-talking DEGs ($degree \geq 2$) and their corresponding $abs(log_2FC)$ values [Fig 5c]. Those include **COL1A2, F2R, FZD4, BCL2L1, CDKN1A, TGFA, MAPK13, THBS1, CDH1,** and **RAC2** [Table 5]. We hypothesize these 10 cross-talking hubs as notable biomarkers in dasatinib resistance, where the first 3 genes are down-regulated, and the remaining are up-regulated in resistant-vs-sensitive conditions, respectively. Moreover, a non-parametric test, i.e., *KolmogorovSmirnov test* revealed that the distribution of $abs(log_2FC)$ values (in resistant-vs-sensitive conditions) for those 9 cross-talking DEGs ($degree \geq 2$) is significantly differ (P-value = 0.000261) from those of non-cross-talking DEGs ($degree = 1$). This may further reinforce that cross-talking, and Hub DEGs are not only perturbed by themselves but also their dysregulation has a cascading effect, perturbing multiple pathways simultaneously. This may significantly contribute to the mechanisms of dasatinib resistance in pancreatic cancer and, therefore, can be defined as highly prioritized biomarkers and novel drug targets.

Signaling Pathway Impact analysis of DEGs demonstrates Pathways with Significant Perturbation Activities

Beyond a mere enrichment test of differentially expressed genes through statistical overlap measurement (i.e., over-representation test), pathway topology analysis may consider the position of genes within a pathway that can identify key signalling genes based on their network centrality and connectivity. To detect the perturbation activities of signalling pathways

bioRxiv preprint doi: https://doi.org/10.64898/2026.02.22.707324; this version posted February 23, 2026. The copyright holder for this preprint (which was not certified by peer review) is the author/funder, who has granted bioRxiv a license to display the preprint in perpetuity. It is made available under a CC-BY 4.0 International license.

based on the frequency of DEGs and their structural dependencies through static protein-protein interactions, we conducted the signalling pathway impact analysis (SPIA) [11]. It observes how a particular pathway reveals signalling perturbation via capturing probabilities of two types of evidence, i.e., the probability of over-representation of DEGs ($pNDE$) (measures the chance of biological irrelevance) and the probability of abnormal perturbation through network topology ($pPERT$) (measures the amount of perturbation in each pathway) against the background. The signaling pathways from the KEGG database were only used to construct an SPIA object which was later used for analysing significant DEGs along with their log2 fold changes (from our previous result). We have used *normal inversion* approach to combine both $p-$values ($pPERT$ and $pNDE$) since it generates the global p-value (i.e., pG) by having a higher emphasis on both $pPERT$ and $pNDE$ being as low as possible (i.e., significant). Note the number of bootstrap iterations, nB, was used as default [i.e., $nB = 2000$]. This p-value is further corrected using both FDR and Bonferroni correction methods as $pGFDR$ and $pGFWER$, respectively. Based on a threshold of $pGFWER < 0.05$, 9 signalling pathways were found to be significantly perturbed in dasatinib resistance [Table 6], including p53, Neurotrophin, Fc epsilon RI, PPAR, WNT, NF-kappa B, MAPK, Rap1, PI3K-Akt signalling pathways. Among these 9 singling pathways, only the $p53$ signalling pathway (KEGG Pathway ID: 04115) demonstrated the most pronounced perturbation ($pPERT = 0.003$) [Figure 6a-c]. Up-regulation of THBS1, CDKN1A, CDKN2A, SFN, BCL2L1, GADD45A, PPP1R13L, CCND1, SERPINB5, and IGFBP3, and down-regulation of CASP8 play crucial downstream roles in controlling/mediating cell cycle arrest, apoptosis, metastasis, and angiogenesis inhibition, DNA damage response, and IGF pathway interactions [Figure 7].

Validating with StringDB and Human Protein Atlas Databases

Identified resistant biomarkers [see Table 5] were further validated using existing knowledge based on StringDB, TCGA gene expression changes from the Human Protein Atlas, and PubMed. Using the StringDB web portal, 10 biomarkers were queried for potential connections among them - revealing an induced subnetwork of 10 nodes (confidence score threshold ≥ 0.4), where average node degree was observed as 1.8 and average local connected components $= 0.633$. This induced subnetwork also exhibited a PPI enrichment P-value $= 0.015$, indicating that the number of observed edges (9 edges) is significantly more than expected (4 edges) for a random gene set with the same size and same degree distribution [Figure 8a]. Interestingly, none of the StringDB connections found among these 10 resistant biomarkers were exhibiting physical protein-protein interactions, but only gene co-expression, co-mentioned in Pubmed abstracts, and homologs interactions in other species. However, functional enrichment of these resistant biomarkers with GO terms (Biological Process), Subcellular localizations (compartments) [see Figure 8b and Figure 8c], Reactome Pathways, WikiPathways, and Pubmed references [Supplementary Figure S1, Supplementary Figure S2, Supplementary Figure S3] revealed highly significant results with FDR-corrected P-value ≤ 0.05 [See Supplementary Table S1]. Without physical connections, such significant functional relevance of these resistant biomarkers encourages us to observe beyond by enlarging the network (with a threshold of no more than 10 interactors) with the aim of identifying actual functional modules. Incidentally, by doing so, two clusters were identified by the MCL clustering algorithm [Figure 8d] - Bladder Cancer (additional genes: MMP2, MMP9, and PTK2) and Pancreatic Cancer (additional genes: AKT2 and AKT3), each having statistically significant PPI enrichment scores, 4.63×10^{-10} and 2.13×10^{-08}, respectively.

A manual literature search with these findings revealed their connections with pancreatic cancer resistance mechanisms. While "Positive regulation of cell population proliferation" is highly relevant with pancreatic cancer resistance [20], its connection with the "Response to oxygen-containing compound" biological process has been multifaceted, which involves hypoxia adaptation [21], Reactive oxygen species (ROS) balance [22, 23], and stromal interactions [24]. Moreover, genes/protein alteration involved in "Endocytic vesicle membrane" compartments may influence drug trafficking and receptor internalization, with RCC1-mediated disruption of nucleocytoplasmic transport impairing metabolic pathways critical for chemotherapy efficacy [25]. The cell surface protein STK33, stabilized by the lncRNA MACC1-AS1, suppresses ferroptosis to evade chemotherapy-induced oxidative damage [26]. Cancer-associated fibroblasts (CAFs) mediate stromal-tumor crosstalk, transferring cytokines like IL-6 and oncogenic miRNAs that drive resistance [27].

Moreover, the resistant biomarkers were also evaluated with their potential coherence with gene (TCGA: The Cancer Genome Atlas) and protein expression (CPTAC: Clinical Proteomic Tumor Analysis Consortium) changes in cancer-vs-normal patients, collected from the Human Protein Atlas (HPA) database [13]. Among 10 biomarkers found in dasatinib resistance, only **RAC1**, **TGFA**, and **BCL2L1** were found prognostic in Pancreatic adenocarcinoma (PAAD) with statistical significance (P-values < 0.001) based on the TCGA gene expression data only [see Supplementary Figure S4].

Tumour-vs-normal comparison of relative protein expression data (nRPX) from CPTAC was conducted using the Wilcoxon test for all the resistant biomarkers, where 2 genes (FZD4 and TGFA) revealed their proteomics data as missing. Among the remaining 8 genes, all the genes demonstrated statistically significant (P-value < 0.001) differential *proteome* abundance in tumours-vs-normal, except F2R, CDKN1A and RAC2 [Figure 9]. Moreover, THBS1, COL1A2, and BCL2L1, were upregulated, whereas MAPK13 and CDH1 were found as down-regulated [Table 7]. Moreover, using RNA expression data from TCGA, only BCL2L1 and TGFA genes were found to be significantly prognostic [Figure 10].

4 | Discussion & Limitations

Drug resistance is a significant threat in cancer treatment where resistant cells' growths can not be controlled despite continuous intake of corresponding drugs. In this study, we analyzed an array-based transcriptomics dataset from dasatinib-sensitive and dasatinib-resistant cell lines to decipher the putative mechanistic details of dasatinib resistance in pancreatic cancer. Here, we conducted an integrated analysis of differential biomarker

bioRxiv preprint doi: https://doi.org/10.64898/2026.02.22.707324; this version posted February 23, 2026. The copyright holder for this preprint (which was not certified by peer review) is the author/funder, who has granted bioRxiv a license to display the preprint in perpetuity. It is made available under a CC-BY 4.0 International license.

identification, functional term and pathway enrichment analysis to identify a tentative list of differential biomarkers and their associated pathways that revealed biological relevance - yielding *p53 signalling* and *FC epsilon RI signalling* pathways as the most significantly enriched. Gene set enrichment analysis (GSEA) identified terms that were predominantly related to pancreatic cancer, which suggests the biological relevance of DEGs in resistant-vs-sensitive conditions. Moreover, an ad-hoc and scale-free topology inducing inter-pathway cross-talk network analysis identified that these two pathways (i.e., *p53 signalling* and *FC epsilon RI signalling*) combinedly drive the overall perturbation by cross-talking with 87% (14 out of 16) all significantly enriched signalling pathways. During the signalling pathway impact analysis (SPIA), these two pathways were also found highly perturbed based on total perturbation accumulation and degree of dysregulation, where their Bonferroni-corrected *P*-values were 3.1×10^{-5}, and 1.8×10^{-2}, respectively [see Table 6].

P53 signalling plays crucial roles in mediating the normal growth of cells and utilizes its tumour-suppressing capability, however, re-programming of its signalling activities significantly facilitates dysregulation of normal cell functions, such as cell growth, apoptosis, DNA damage repair, and metabolism, which may infer resistance to dasatinib therapy [28, 29]. Regarding the FC epsilon RI (a high-affinity receptor of IgE) signalling, some literature suggests that the angiogenesis in pancreatic cancer can be induced by the inflammation caused within tumour micro-environment [30, 31]. However, the role of *FC epsilon RI signalling* activities in pancreatic cancer is poorly understood [32]. In our study, several genes in this pathway are differentially regulated that are responsible for pancreatic cancer metastasis and/or resistance to therapies including LYN [33], FYN [34, 35], RAC1 and RAC2 [36], MAPK13 [6].

Those two pathways managed to disseminate their perturbations globally via 13 cross-talking DEGs ($degree \geq 2$), among which 5 of them showed higher degree of dysregulation ($abs(log_2FC) \geq 2$) in dasatinib resistance cell lines, including **THBS1**, **CDKN1A**, **BCL2L1**, **RAC2**, and **MAPK13**. THBS1 expression was found to be highly upregulated in pancreatic cancer cells, knockdown of which suppresses the pancreatic cancer progression in nude mice [37]. The cyclin-dependent kinase inhibitor p21 (CDKN1A) has multifaceted (dual-role) and context-dependent roles, including both tumour-suppressing and potential Pro-tumorigenic roles [38]. Alexandros *et al.* suggested that in p53 deficient micro-environment, p21 may play oncogenic roles depending on its subcellular localization [38]. Interestingly, in this study, we found the downregulation of TP53 ($log2FC = -0.55$) and BCL2 associated genes (BAD: $log2FC = -0.67$, BCLAF1: $log2FC = -0.27$, BAG2: $log2FC = -0.23$, BAG3: $log2FC = -0.67$, and BAG6: $log2FC = -0.4$) and the upregulation of MDM2 ($log2FC = 0.37$) in resistant-vs-sensitive cell lines, which indicate the overall downregulation of p53 signalling pathway. Moreover, the SPIA (Signalling Pathway Impact Analysis) results have independently identified the p53 signalling pathway as "*Inhibited*", together which may suggest that p21 (CDKN1A) may acquire an oncogenic role in pancreatic cancer in resistance condition by inhibiting apoptosis and promoting abnormal cell growth [38]. Moreover, CDKN1A upregulation has been observed in cisplatin-pemetrexed chemoresistance in non-small cell lung cancer cells [39].

Over-expression of BCL2L1 was observed in pancreatic cancer patients [40], and it also induces resistance to several treatments, including gemcitabine, 5FU, and niraparib, in the pancreatic cancer cell line, AsPC-1 [41]. RAC2 promotes the tumour growth and metastasis [42], and activated RAC2 GTPase mediates Perineural invasion and metastasis in pancreatic cancer via MUC21 phosphorylation [43]. MAPK13 (p38 δ) is a member of the mitogen-activated protein kinase (MAPK) family, which works as a cross-talking signalling hub and plays crucial roles in cell proliferation, transcription regulation and differentiation. Godfrey *et al.* has reported that, due to epigenetic reprogramming of DNA hypermethylation, cells acquire resistance to MAPK signalling inhibitors in pancreatic cancer [6].

Identifying and analysing cross-talks among highly active signalling pathways can facilitate better mechanistic details underlying any disease context. To underscore the systemic nature of resistance mechanisms, here in this study, we modelled the signalling cross-talk network as a gene-pathway association, where the nodes are either DEGs or enriched signalling pathways where they belong and the edges were defined with the gene-pathway associations from known annotations, e.g., KEGG [Figure 4]. Therefore, cross-talking nodes were only those DEGs that were connecting at least two signalling pathways, and non-cross-talking DEGs were otherwise. For instance, p53 signallings cross-talk with pathways like ErbB, Wnt, and PI3K-Akt via key upregulated genes such as CDKN1A and BCL2L1 suggests its central role in orchestrating cellular responses to Dasatinib.

Note, Figure 4 shows only the pruned version of that network, where the DEG nodes that have a degree of connectivity as 1, were hidden as they weren't effectively defined as cross-talking DEGs. Again, although this cross-talk network is constructed in an ad-hoc manner, we urge that it manifests biological significance since the gene-pathway membership edges indirectly map some meaningful biological connections (e.g., protein-protein interactions). Similar claim can be made based on the observation of its scale-free topology [Figure 5a-b] and the correlation of the degree of connectivity (i.e., node degree) and the degree of dysregulation ($abs(log_2FC) \geq 2$) for the cross-talking hubs [Figure 5c-d]. Since the cross-talking DEGs offer compensatory pathway activations contributing to the drug resistance phenomenon [8], detecting and targeting those are very crucial for novel therapeutics design.

This study possesses several limitations. Firstly, we have used transcriptomics dataset only for discovering biomarkers in acquired dasatinib resistance (ADR), which may not fully reveal post-transcriptional or post-translational interactions among signaling proteins or molecules in that context. Secondly, proposed the cross-talk network model only relates the context with a static gene-pathway association, which may ignore dynamic scenario within tumor micro-environment. Moreover, cell-line derived transcriptomics datasets may also not capture the ADR mechanisms *in vivo* settings. To overcome these limitations, we aim to integrated multi-omics datasets, including proteomics and metabolomics data to capture more comprehensive details of ADR mechanims in pancreatic cancer. Moreover, time-course data, single-cell, or spatial transcriptomics data can also be integrated to reveal dynamic cell-cell or pathway-pathway communications for better cross-talk network modeling in ADR. Finally, additional *in vivo* based experimental validation may strengthen the findings of ADR biomarkers in pancreatic cancer.

bioRxiv preprint doi: https://doi.org/10.64898/2026.02.22.707324; this version posted February 23, 2026. The copyright holder for this preprint (which was not certified by peer review) is the author/funder, who has granted bioRxiv a license to display the preprint in perpetuity. It is made available under a CC-BY 4.0 International license.

5 | Conclusions

In this study, we systematically addressed our core research questions by identifying dysregulated signalling molecules in dasatinib-resistant versus sensitive pancreatic cancer cell lines, interrogating their coordinated cross-talk across enriched pathways, and pinpointing dominant drivers of global perturbation. Through integrated differential expression profiling, enrichment analyses, signalling cross-talk network modelling, and topology-aware SPIA, we demonstrate that p53 and Fc-RI signalling axes act as complementary and dominant perturbation disseminators, collectively coordinating 87% of enriched pathway cross-talk. Scale-free topology analysis further prioritized ten cross-talking hub biomarkersmost notably BCL2L1, RAC2, MAPK13, THBS1, and CDKN1Awhose dysregulation correlates with network centrality and resistance-associated signalling cascades. Multi-layer validation using TCGA, CPTAC, and StringDB supports their biological and prognostic relevance. While the study is limited by reliance on in vitro transcriptomic models and pathway annotations that do not capture dynamic temporal rewiring or direct causal interactions, the convergence of statistical, topological, and biological evidence strengthens the robustness of our findings. Future work should incorporate single-cell and phosphoproteomic profiling, functional perturbation assays, and drug-combination validation to experimentally confirm these network vulnerabilities and enable rational design of next-generation therapeutic strategies targeting resistance dissemination rather than isolated molecular events.

Data and code availability

- Gene expression data of dasatinib-resistant and dasatinib-sensitive pancreatic cancer cell lines are collected from Gene Expression Omnibus (GEO) under the accession number: GSE59357.
- All original code has been deposited at Zenodo (https://doi.org/10.5281/zenodo.14954417).

Author Contributions

Conceptualization, A.A.; methodology, A.A.; investigation, A.A.; writing-original draft, A.A.; writing-review & editing, A.A. and M.A.M.; funding acquisition, M.A.M. and M.J.A.S.; resources, A.A.; supervision, M.A.M., and M.J.A.S.

Acknowledgments

We thank Dr. Guangchuang (YuLabSMU) for his excellent R package: clusterprofiler, as some parts of the network visualization code in our work have been reproduced/inspired by that package.

Conflicts of Interest

The authors declare no conflicts of interest.

References

1. Rebecca L. Siegel, Tyler B. Kratzer, Angela N. Giaquinto, Hyuna Sung,, and Ahmedin Jemal. "Cancer statistics, 2025." *CA: A Cancer Journal for Clinicians* 75, no. 1 (2025): 1045.
2. Francisco Quiñonero, Cristina Mesas, Kevin Doello, Laura Cabeza, Gloria Perazzoli, Cristina Jimenez-Luna, Ana Rosa Rama, Consolación Melguizo,, and Jose Prados. "The challenge of drug resistance in pancreatic ductal adenocarcinoma: a current overview." *Cancer Biology amp; Medicine* 16, no. 4 (2019): 688699.
3. Wenwen Chien, Qiao-Yang Sun, Kian Leong Lee, Ling-Wen Ding, Peer Wuensche, Lucia A. Torres-Fernandez, Siew Zhuan Tan, Itay Tokatly, Norazean Zaiden, Lorenz Poellinger, Seiichi Mori, Henry Yang, Jeffrey W. Tyner,, and H. Phillip Koeffler. "Activation of protein phosphatase 2A tumor suppressor as potential treatment of pancreatic cancer." *Molecular Oncology* 9, no. 4 (2015): 889905.
4. Dong Wook Je, Young Moon O, Young Geon Ji, Yunkyung Cho,, and Dong Hyeon Lee. "The Inhibition of Src Family Kinase Suppresses Pancreatic Cancer Cell Proliferation, Migration, and Invasion." *Pancreas* 43, no. 5 (2014): 768776.
5. Tobias Bartscht, Benjamin Rosien, Dirk Rades, Roland Kaufmann, Harald Biersack, Hendrik Lehnert, Frank Gieseler,, and Hendrik Ungefroren. "Dasatinib blocks transcriptional and promigratory responses to transforming growth factor-beta in pancreatic adenocarcinoma cells through inhibition of Smad signalling: implications for in vivo mode of action." *Molecular Cancer* 14, no. 1.
6. Laura K Godfrey, Jan Forster, Sven-Thorsten Liffers, Christopher Schröder, Johannes Köster, Leonie Henschel, Kerstin U Ludwig, David Lähnemann, Marija Trajkovic-Arsic, Diana Behrens, Aldo Scarpa, Rita T Lawlor, Kathrin E Witzke, Barbara Sitek, Steven A Johnsen, Sven Rahmann, Bernhard Horsthemke, Michael Zeschnigk,, and Jens T Siveke. "Pancreatic cancer acquires resistance to MAPK pathway inhibition by clonal expansion and adaptive DNA hypermethylation." *Clin. Epigenetics* 16, no. 1 (2024): 13.
7. Mara H. Sherman, and Gregory L. Beatty. "Tumor Microenvironment in Pancreatic Cancer Pathogenesis and Therapeutic Resistance." *Annual Review of Pathology: Mechanisms of Disease* 18, no. 1 (2023): 123148.
8. AKM Azad, Alfons Lawen,, and Jonathan M Keith. "Prediction of signaling cross-talks contributing to acquired drug resistance in breast cancer cells by Bayesian statistical modeling." *BMC Systems Biology* 9, no. 1.
9. A. K. M. Azad, Alfons Lawen,, and Jonathan M. Keith. "Bayesian model of signal rewiring reveals mechanisms of gene dysregulation in acquired drug resistance in breast cancer." *PLOS ONE* 12, no. 3 (2017): e0173331.
10. "KEGG PATHWAY Database — genome.jp." https://www.genome.jp/kegg/pathway.html, [Accessed 20-01-2025].
11. Adi Laurentiu Tarca, Sorin Draghici, Purvesh Khatri, Sonia S. Hassan, Pooja Mittal, Jung-sun Kim, Chong Jai Kim, Juan Pedro Kusanovic,, and Roberto Romero. "A novel signaling pathway impact analysis." *Bioinformatics* 25, no. 1 (2008): 7582.
12. Damian Szklarczyk, Rebecca Kirsch, Mikaela Koutrouli, Katerina Nastou, Farrokh Mehryary, Radja Hachilif, Annika L Gable, Tao Fang, NadezhdaăT Doncheva, Sampo Pyysalo, Peer Bork, LarsăJ Jensen,, and Christian vonăMering. "The STRING database in 2023: proteinprotein association networks and functional enrichment analyses for any sequenced genome of interest." *Nucleic Acids Research* 51, no. D1 (2022): D638D646.
13. Mathias Uhlén, Linn Fagerberg, Björn M. Hallström, Cecilia Lindskog, Per Oksvold, Adil Mardinoglu, Åsa Sivertsson, Caroline Kampf, Evelina Sjöstedt, Anna Asplund, IngMarie Olsson, Karolina Edlund, Emma Lundberg, Sanjay Navani, Cristina Al-Khalili Szigyarto, Jacob Odeberg, Dijana Djureinovic, Jenny Ottosson Takanen, Sophia Hober, Tove Alm, Per-Henrik Edqvist, Holger Berling, Hanna Tegel, Jan Mulder, Johan Rockberg, Peter Nilsson, Jochen M. Schwenk, Marica Hamsten, Kalle von Feilitzen, Mattias Forsberg, Lukas Persson, Fredric Johansson, Martin Zwahlen, Gunnar von Heijne, Jens Nielsen,, and Fredrik Pontén. "Tissue-based map of the human proteome." *Science* 347, no. 6220.
14. Indrajeet Patil. "Visualizations with statistical details: The 'ggstatsplot' approach." *Journal of Open Source Software* 6, no. 61

bioRxiv preprint doi: https://doi.org/10.64898/2026.02.22.707324; this version posted February 23, 2026. The copyright holder for this preprint (which was not certified by peer review) is the author/funder, who has granted bioRxiv a license to display the preprint in perpetuity. It is made available under a CC-BY 4.0 International license.

(2021): 3167.

15. T.R.J. Evans, E. Van Cutsem, M.J. Moore, I.S. Bazin, A. Rosemurgy, G. Bodoky, G. Deplanque, M. Harrison, B. Melichar, D. Pezet, A. Elekes, E. Rock, C. Lin, L. Strauss,, and P.J. ODwyer. "Phase 2 placebo-controlled, double-blind trial of dasatinib added to gemcitabine for patients with locally-advanced pancreatic cancer." *Annals of Oncology* 28, no. 2 (2017): 354361.
16. Marilyn Kaul, Ahmed Y. Sanin, Wenjie Shi, Christoph Janiak,, and Ulf D. Kahlert. "Nanoformulation of dasatinib cannot overcome therapy resistance of pancreatic cancer cells with low LYN kinase expression." *Pharmacological Reports* 76, no. 4 (2024): 793806.
17. A.K.M. Azad. "rXTalkViz: A R package to quantify, visualize, and report carcinogenic footprints of functional pathway crosstalks." *Software Impacts*22 (2024): 100708.
18. A.K.M. Azad, Alfons Lawen,, and Jonathan M. Keith. 2018. "Cross-Talk Categorisations in Data-Driven Models of Signalling Networks: A System-Level View." In *Gene Expression and Regulation in Mammalian Cells*, , edited by Fumiaki Uchiumi, Rijeka: IntechOpen.
19. Eivind Almaas, Alexei Vázquez,, and Albert-László Barabási. 2007, December). *SCALE-FREE NETWORKS IN BIOLOGY*, pp. 119. WORLD SCIENTIFIC.
20. Marvin Schober, Ralf Jesenofsky, Ralf Faissner, Cornelius Weidenauer, Wolfgang Hagmann, Patrick Michl, Rainer Heuchel, Stephan Haas,, and J.-Matthias Löhr. "Desmoplasia and Chemoresistance in Pancreatic Cancer." *Cancers* 6, no. 4 (2014): 21372154.
21. Yu Chen, Jialun Wang, Ying Huang, Jianzhuang Wu, Yue Wang, Aotian Chen, Qiyuan Guo, Yixuan Zhang, Shu Zhang, Lei Wang, Xiaoping Zou,, and Xihan Li. "An oncolytic system produces oxygen selectively in pancreatic tumor cells to alleviate hypoxia and improve immune activation." *Pharmacological Research*199 (2024): 107053.
22. Lun Zhang, Jiahui Li, Liang Zong, Xin Chen, Ke Chen, Zhengdong Jiang, Ligang Nan, Xuqi Li, Wei Li, Tao Shan, Qingyong Ma,, and Zhenhua Ma. "Reactive Oxygen Species and Targeted Therapy for Pancreatic Cancer." *Oxidative Medicine and Cellular Longevity* 2016, no. 1.
23. Mingming Xiao, Jing Yang, Mingwei Dong, Xiaoqi Mao, Haoqi Pan, Yalan Lei, Xuhui Tong, Xiaoning Yu, Xianjun Yu,, and Si Shi. "NLRP4 renders pancreatic cancer resistant to olaparib through promotion of the DNA damage response and ROS-induced autophagy." *Cell Death amp; Disease* 15, no. 8.
24. Shahram Parvaneh, Vanda Miklós, Zoltán Gábor Páhi, Diána Szcs, Tamás Monostori, Szilárd Póliska, Viktória Venglovecz, Tibor Pankotai, Lajos Kemény,, and Zoltán Veréb. "Chemoresistance in Pancreatic Cancer: The Role of Adipose-Derived Mesenchymal Stem Cells and Key Resistance Genes." *International Journal of Molecular Sciences* 26, no. 1 (2025): 390.
25. Sahar F. Bannoura, Amro Aboukameel, Husain Yar Khan, Md Hafiz Uddin, Hyejeong Jang, Eliza W Beal, Amalraj Thangasamy, Yang Shi, Seongho Kim, Kay-Uwe Wagner, Rafic Beydoun, Bassel F. El-Rayes, Philip A. Philip, Ramzi M. Mohammad, Muhammad Wasif Saif, Mohammed Najeeb Al-Hallak, Boris C. Pasche,, and Asfar S. Azmi. "RCC1 regulation of subcellular protein localization via Ran GTPase drives pancreatic ductal adenocarcinoma growth." *Cancer Letters*604 (2024): 217275.
26. Jiyun Zhu, Zehao Yu, Xuguang Wang, Jinghui Zhang, Yi Chen, Kaibo Chen, Bin Zhang, Jianhong Sun, Jianshuai Jiang,, and Siming Zheng. "LncRNA MACC1-AS1 induces gemcitabine resistance in pancreatic cancer cells through suppressing ferroptosis." *Cell Death Discovery* 10, no. 1.
27. Carina Shiau, Jingyi Cao, Dennis Gong, Mark T. Gregory, Nicholas J. Caldwell, Xunqin Yin, Jae-Won Cho, Peter L. Wang, Jennifer Su, Steven Wang, Jason W. Reeves, Tae Kyung Kim, Youngmi Kim, Jimmy A. Guo, Nicole A. Lester, Jung Woo Bae, Ryan Zhao, Nathan Schurman, Jamie L. Barth, Maria L. Ganci, Ralph Weissleder, Tyler Jacks, Motaz Qadan, Theodore S. Hong, Jennifer Y. Wo, Hannah Roberts, Joseph M. Beechem, Carlos Fernandez-del Castillo, Mari Mino-Kenudson, David T. Ting, Martin Hemberg,, and William L. Hwang. "Spatially resolved analysis of pancreatic cancer identifies therapy-associated remodeling of the tumor microenvironment." *Nature Genetics* 56, no. 11 (2024): 24662478.
28. Aixin Ou, Xiangxuan Zhao,, and Zaiming Lu. "The potential roles of p53 signaling reactivation in pancreatic cancer therapy." *Biochim. Biophys. Acta Rev. Cancer* 1877, no. 1 (2022): 188662.
29. Jennifer P Morton, Paul Timpson, Saadia A Karim, Rachel A Ridgway, Dimitris Athineos, Brendan Doyle, Nigel B Jamieson, Karin A Oien, Andrew M Lowy, Valerie G Brunton, Margaret C Frame, T R Jeffry Evans,, and Owen J Sansom. "Mutant p53 drives metastasis and overcomes growth arrest/senescence in pancreatic cancer." *Proc. Natl. Acad. Sci. U. S. A.* 107, no. 1 (2010): 246–251.
30. Matthew J Strouch, Eric C Cheon, Mohammad R Salabat, Seth B Krantz, Elias Gounaris, Laleh G Melstrom, Surabhi Dangi-Garimella, Edward Wang, Hidayatullah G Munshi, Khashayarsha Khazaie,, and David J Bentrem. "Crosstalk between mast cells and pancreatic cancer cells contributes to pancreatic tumor progression." *Clin. Cancer Res.* 16, no. 8 (2010): 2257–2265.
31. I Esposito, M Menicagli, N Funel, F Bergmann, U Boggi, F Mosca, G Bevilacqua,, and D Campani. "Inflammatory cells contribute to the generation of an angiogenic phenotype in pancreatic ductal adenocarcinoma." *J. Clin. Pathol.* 57, no. 6 (2004): 630–636.
32. Peng Wei, Hongwei Tang,, and Donghui Li. "Insights into pancreatic cancer etiology from pathway analysis of genome-wide association study data." *PLoS One* 7, no. 10 (2012): e46887.
33. Lazaro E Aira, Elodie Villa, Pascal Colosetti, Parvati Gamas, Laurie Signetti, Sandrine Obba, Emma Proics, Fabien Gautier, Béatrice Bailly-Maitre, Arnaud Jacquel, Guillaume Robert, Frédéric Luciano, Philippe P Juin, Jean-Ehrland Ricci, Patrick Auberger,, and Sandrine Marchetti. "The oncogenic tyrosine kinase Lyn impairs the pro-apoptotic function of Bim." *Oncogene* 37, no. 16 (2018): 2122–2136.
34. Zhi-Yu Chen, Lei Cai, Ping Bie, Shu-Guang Wang, Yan Jiang, Jia-Hong Dong,, and Xiao-Wu Li. "Roles of Fyn in pancreatic cancer metastasis." *J. Gastroenterol. Hepatol.* 25, no. 2 (2010): 293–301.
35. Daniel Elias, and Henrik J Ditzel. "Fyn is an important molecule in cancer pathogenesis and drug resistance." *Pharmacol. Res.*100 (2015): 250–254.
36. Paula Colón-Bolea, Rocío García-Gómez,, and Berta Casar. "RAC1 activation as a potential therapeutic option in metastatic cutaneous melanoma." *Biomolecules* 11, no. 11 (2021): 1554.
37. Ping Li, Kaixuan Wang, Jian Song, Zhuang Chen, Yongyu Li,, and Zhaowei Chen. "THBS1 knockdown suppresses pancreatic cancer progression through JAK2/STAT3 signaling pathway." *Mol. Cell. Probes* 79, no. 102003 (2024): 102003.
38. Alexandros G Georgakilas, Olga A Martin,, and William M Bonner. "P21: A two-faced genome guardian." *Trends Mol. Med.* 23, no. 4 (2017): 310–319.
39. Alice Zamagni, Alice Pasini, Francesca Pirini, Sara Ravaioli, Emanuele Giordano, Anna Tesei, Daniele Calistri, Paola Ulivi, Francesco Fabbri, Flavia Foca, Angelo Delmonte,, and Chiara Molinari. "CDKN1A upregulation and cisplatinpemetrexed resistance in nonsmall cell lung cancer cells." *Int. J. Oncol.* 56, no. 6 (2020): 1574–1584.
40. Dimitrios E Magouliotis, Anna P Karamolegkou, Prokopis-Andreas Zotos, Evangelos Tatsios, Athina A Samara, Dimitra Alexopoulou, Fani Koutsougianni, Nikos Sakellaridis, Dimitris Zacharoulis,, and Konstantinos Dimas. "Bioinformatic analysis of the BCL-xL/BCL2L1 interactome in patients with pancreatic cancer." *Medicina (Kaunas)* 58, no. 11 (2022): 1663.

bioRxiv preprint doi: https://doi.org/10.64898/2026.02.22.707324; this version posted February 23, 2026. The copyright holder for this preprint (which was not certified by peer review) is the author/funder, who has granted bioRxiv a license to display the preprint in perpetuity. It is made available under a CC-BY 4.0 International license.

41. Dinesh Thummuri, Sajid Khan, Patrick W Underwood, Peiyi Zhang, Janet Wiegand, Xuan Zhang, Vivekananda Budamagunta, Amin Sobh, Abderrahmane Tagmount, Alexander Loguinov, Andrea N Riner, Ashwin S Akki, Elizabeth Williamson, Robert Hromas, Christopher D Vulpe, Guangrong Zheng, Jose G Trevino,, and Daohong Zhou. "Overcoming gemcitabine resistance in pancreatic cancer using the BCL-XL-specific degrader DT2216." *Mol. Cancer Ther.* 21, no. 1 (2022): 184–192.
42. Shweta Joshi, Alok R Singh, Muamera Zulcic, Lei Bao, Karen Messer, Trey Ideker, Janusz Dutkowski,, and Donald L Durden. "Rac2 controls tumor growth, metastasis and M1-M2 macrophage differentiation in vivo." *PLoS One* 9, no. 4 (2014): e95893.
43. Yutong Chen, Weiyu Zhang, Yan Zeng, Pengfei Yang, Yaning Li, Xinyue Liang, Kecheng Liu, Hai Lin, Yalan Dai, Jiancong Zhou, Bingqi Hou, Zhenting Ma, Yujing Lin, Wenzheng Pang,, and Linjuan Zeng. "GDNF-induced phosphorylation of MUC21 promotes pancreatic cancer perineural invasion and metastasis by activating RAC2 GTPase." *Oncogene* 43, no. 34 (2024): 2564–2577.
44. Karunakar Pothuganti. "Long Short-Term Memory (LSTM) algorithm based prediction of stock market exchange." *International Journal of Research Publication and Reviews* 2, no. 1 (2021): 90–93.

Supporting Information

Supplementary Figure S1, Supplementary Figure S2, Supplementary Figure S3, Supplementary Figure S4 and their legends in the supplementary files PDF

Supplementary Table S1. Full spreadsheet of differential expression of Resistant-VS-Sensitive pancreatic cancer cell lines.

bioRxiv preprint doi: https://doi.org/10.64898/2026.02.22.707324; this version posted February 23, 2026. The copyright holder for this preprint (which was not certified by peer review) is the author/funder, who has granted bioRxiv a license to display the preprint in perpetuity. It is made available under a CC-BY 4.0 International license.

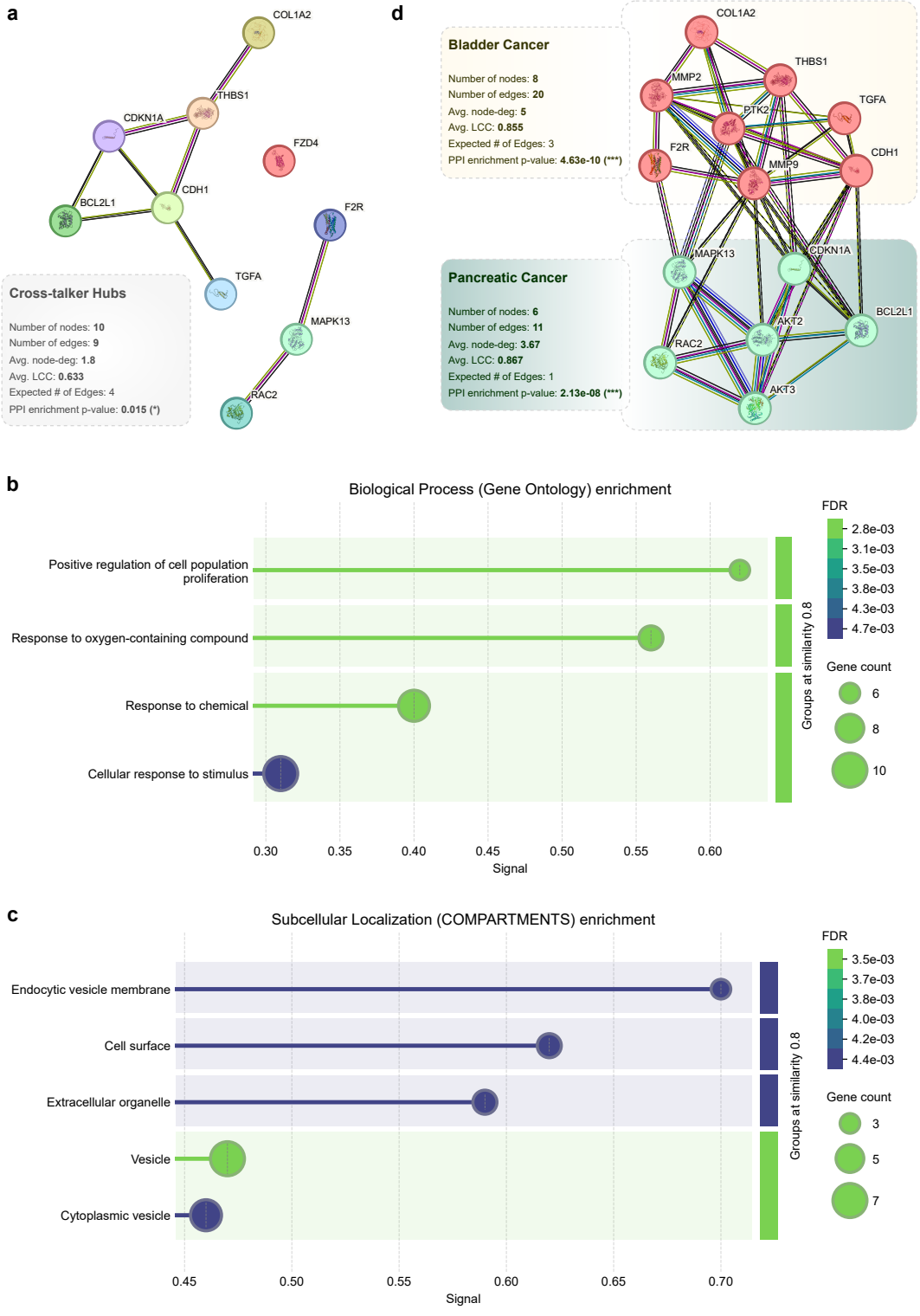


FIGURE 8 | StringDB validation of 10 cross-talking biomarkers in Dasatinib resistance. (a) Protein-Protein interactions among cross-talking hubs (confidence score ≥ 0.4). Enrichment of 10 cross-talking biomarkers with **(b)** GO term enrichment (Biological Process) and **(c)** Subcellular localizations (compartments), indicating additional evidence and localized roles of these biomarkers in dasatinib resistance. **(d)** With augmented nodes and their incident connections from StringDB, an MCL clustering yielded two clusters, cluster-1: *Bladder cancer* (8 genes), and cluster-2: *Pancreatic cancer* (6 genes), each having statistically significant PPI enrichment scores.

bioRxiv preprint doi: https://doi.org/10.64898/2026.02.22.707324; this version posted February 23, 2026. The copyright holder for this preprint (which was not certified by peer review) is the author/funder, who has granted bioRxiv a license to display the preprint in perpetuity. It is made available under a CC-BY 4.0 International license.

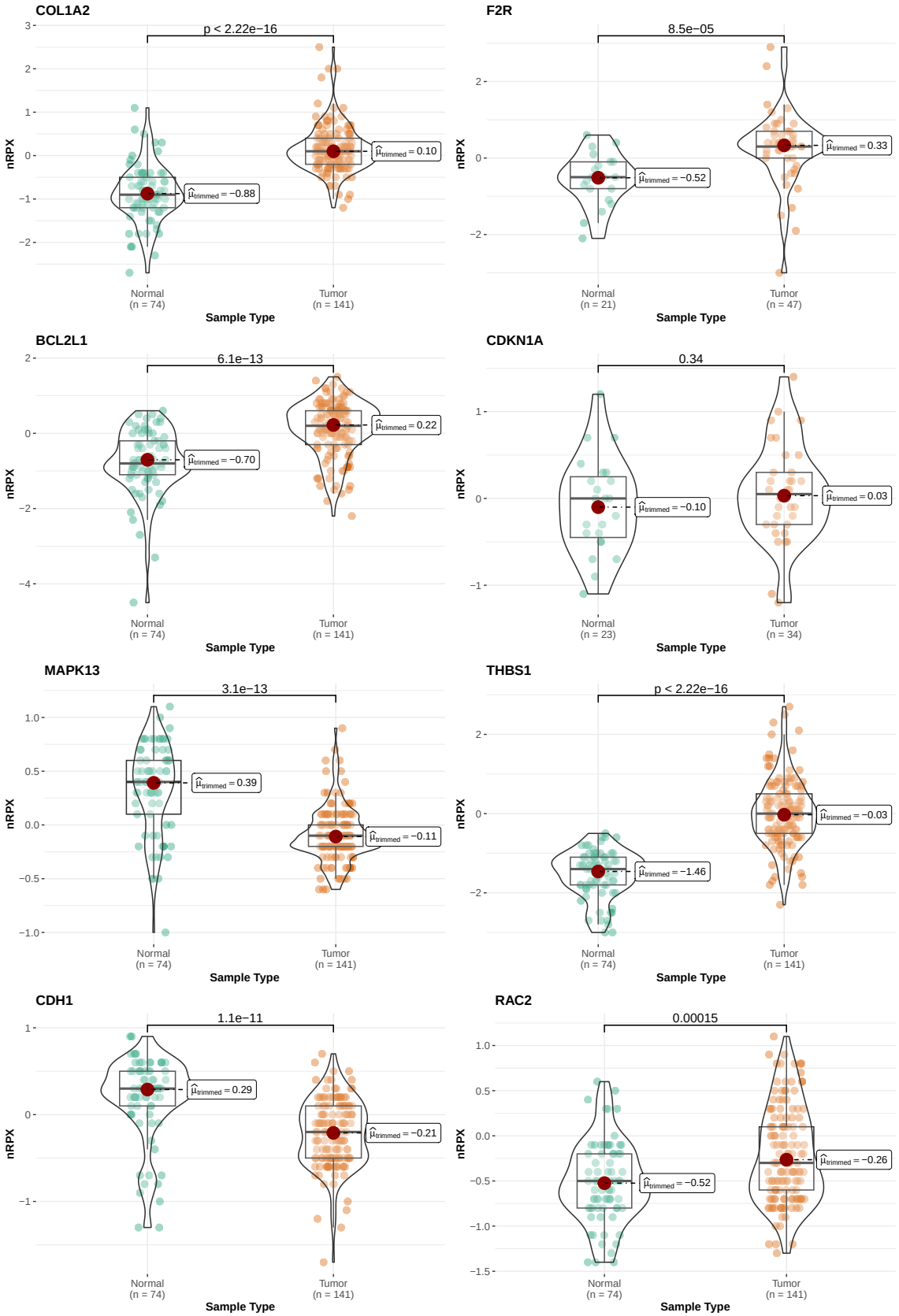


FIGURE 9 | CPTAC relative proteomics validation of 8 or 10 resistant biomarkers. Most of the biomarkers (Except CDKN1A) were found to be significantly dysregulated (Wilcoxon test) in Pancreatic adenocarcinoma (PAAD) in Tumor-vs-Normal relative protein express (nRPX). Note 2 other genes, FZD4 and TGFA, weren't found with any expression data.

bioRxiv preprint doi: https://doi.org/10.64898/2026.02.22.707324; this version posted February 23, 2026. The copyright holder for this preprint (which was not certified by peer review) is the author/funder, who has granted bioRxiv a license to display the preprint in perpetuity. It is made available under a CC-BY 4.0 International license.

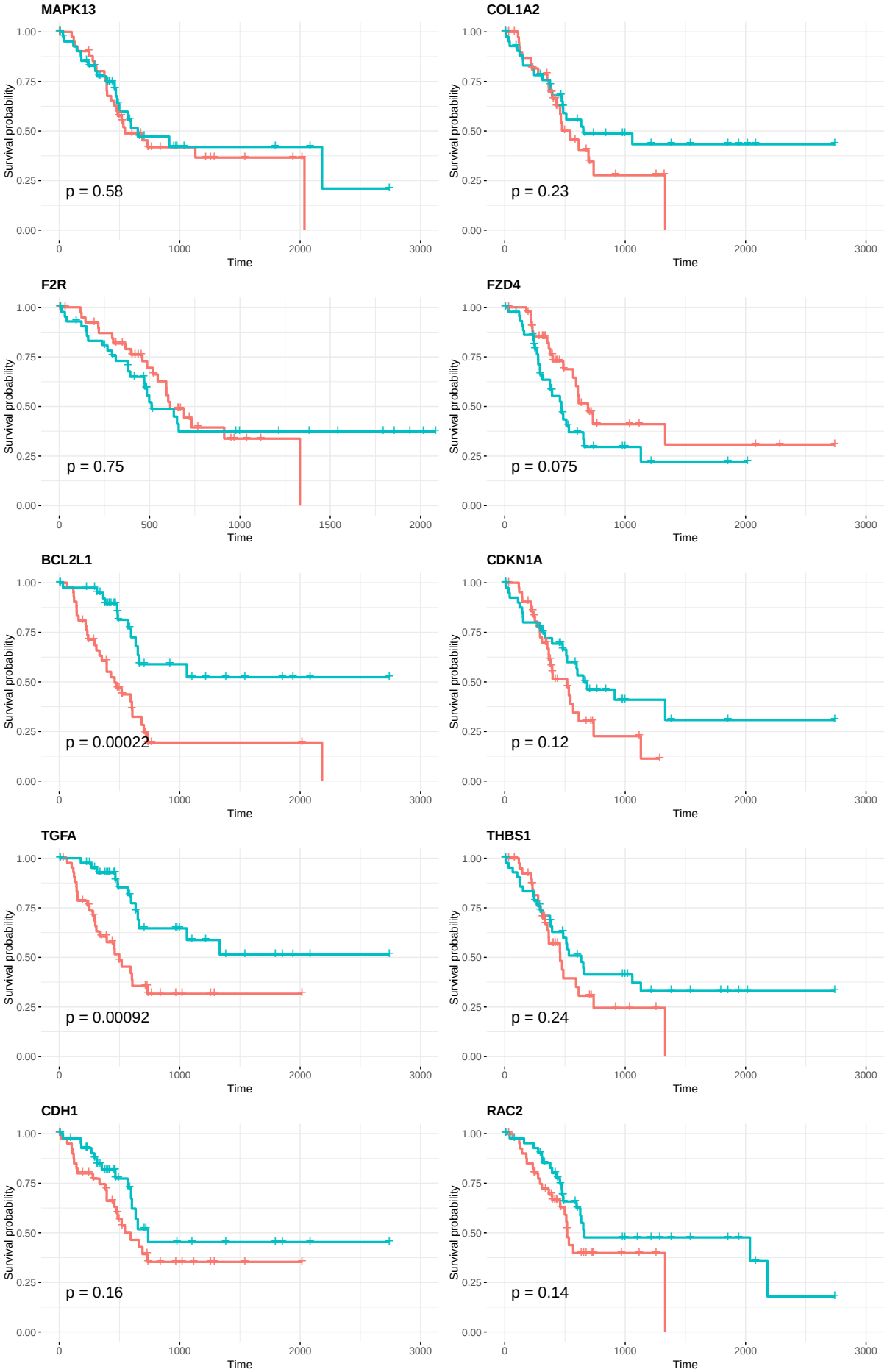
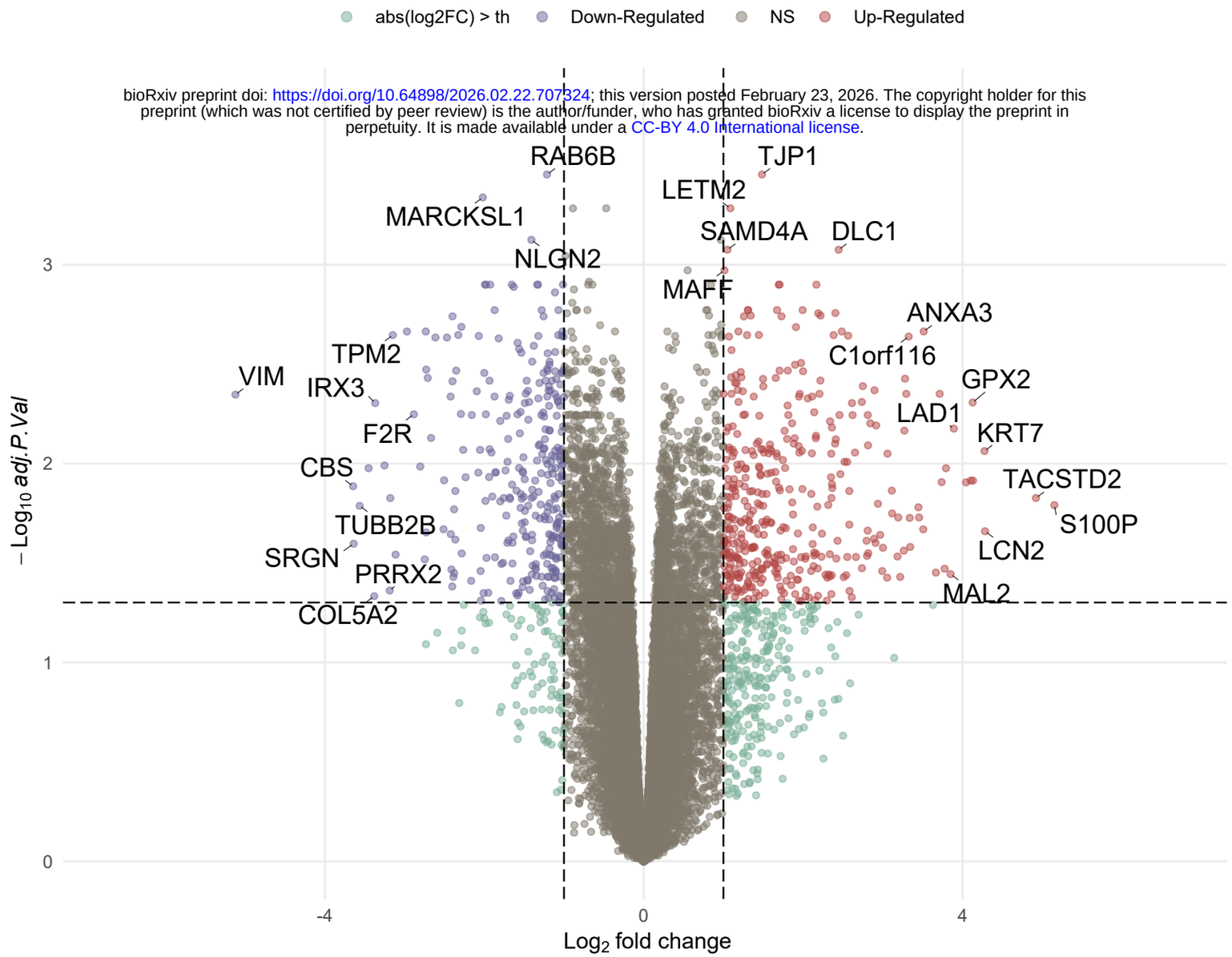


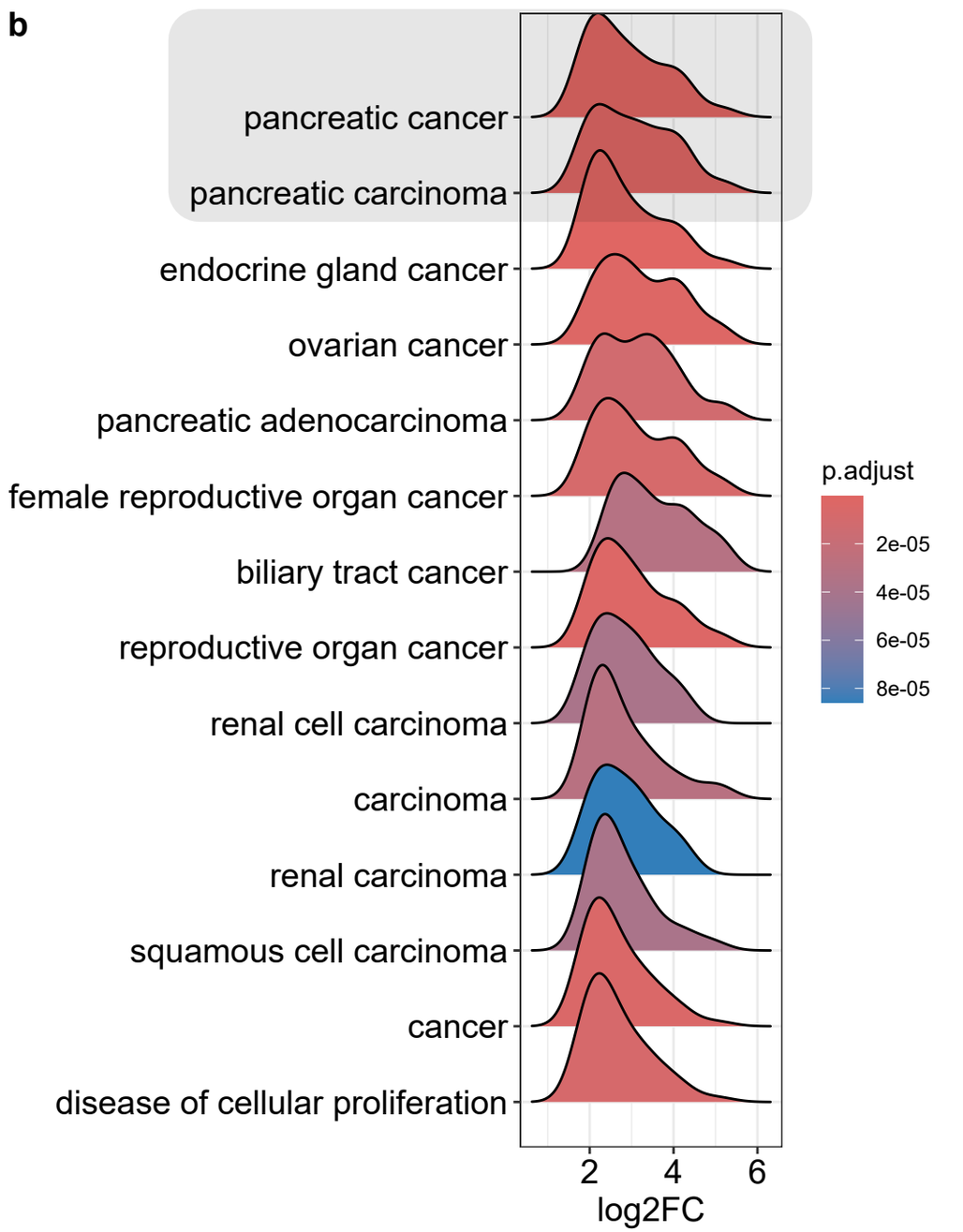
FIGURE 10 | TCGA (RNA expression) validation 10 resistant biomarkers. Survival analysis was conducted using the Cox regression model.

bioRxiv preprint doi: https://doi.org/10.64898/2026.02.22.707324; this version posted February 23, 2026. The copyright holder for this preprint (which was not certified by peer review) is the author/funder, who has granted bioRxiv a license to display the preprint in perpetuity. It is made available under a CC-BY 4.0 International license.

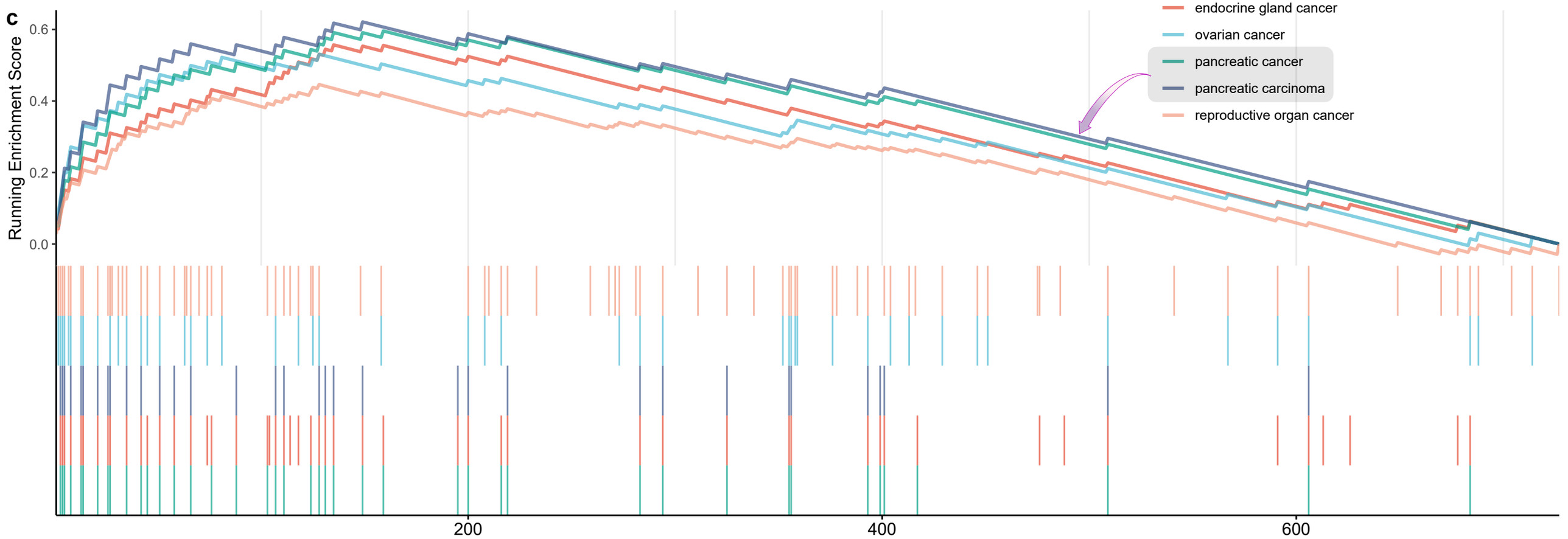
a



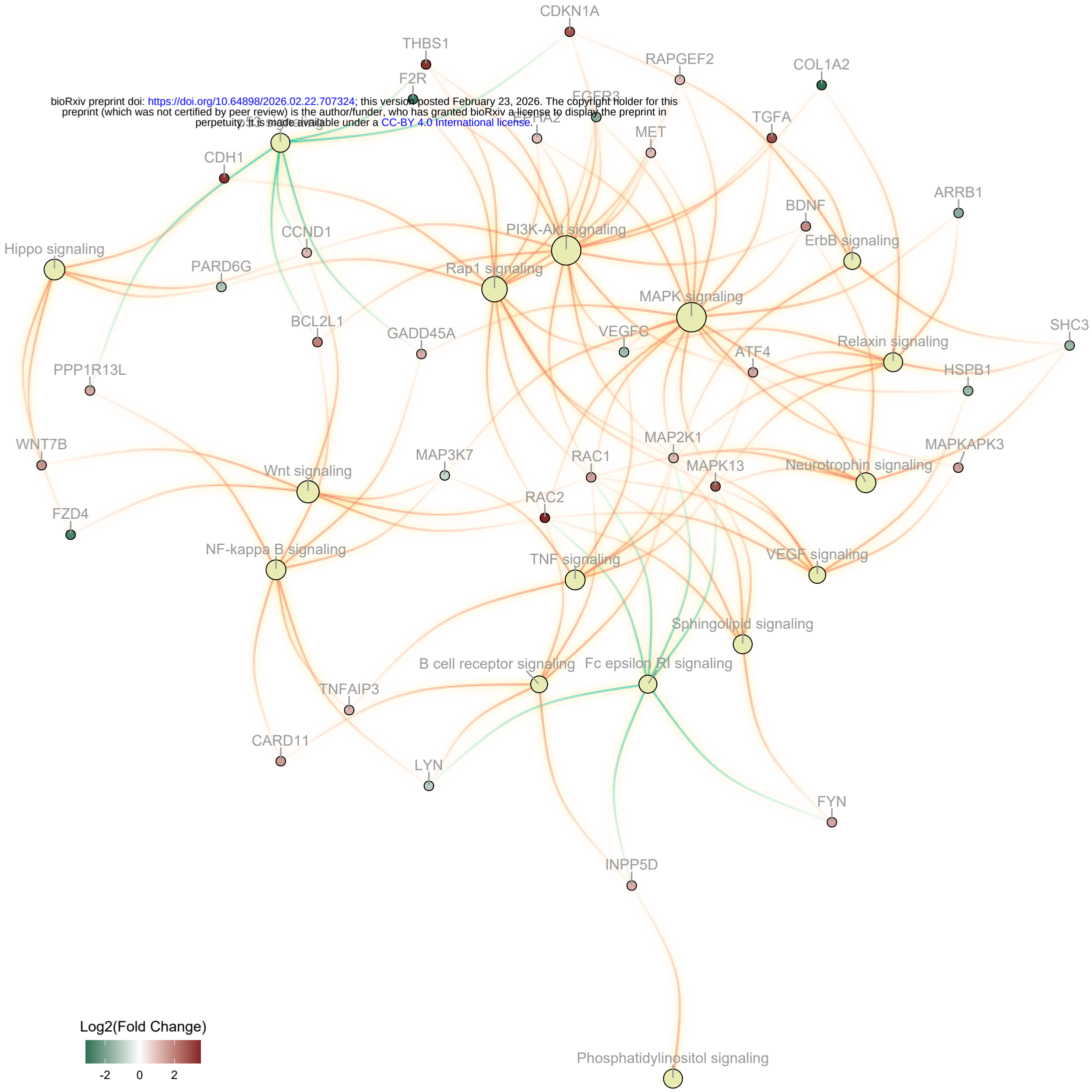
b

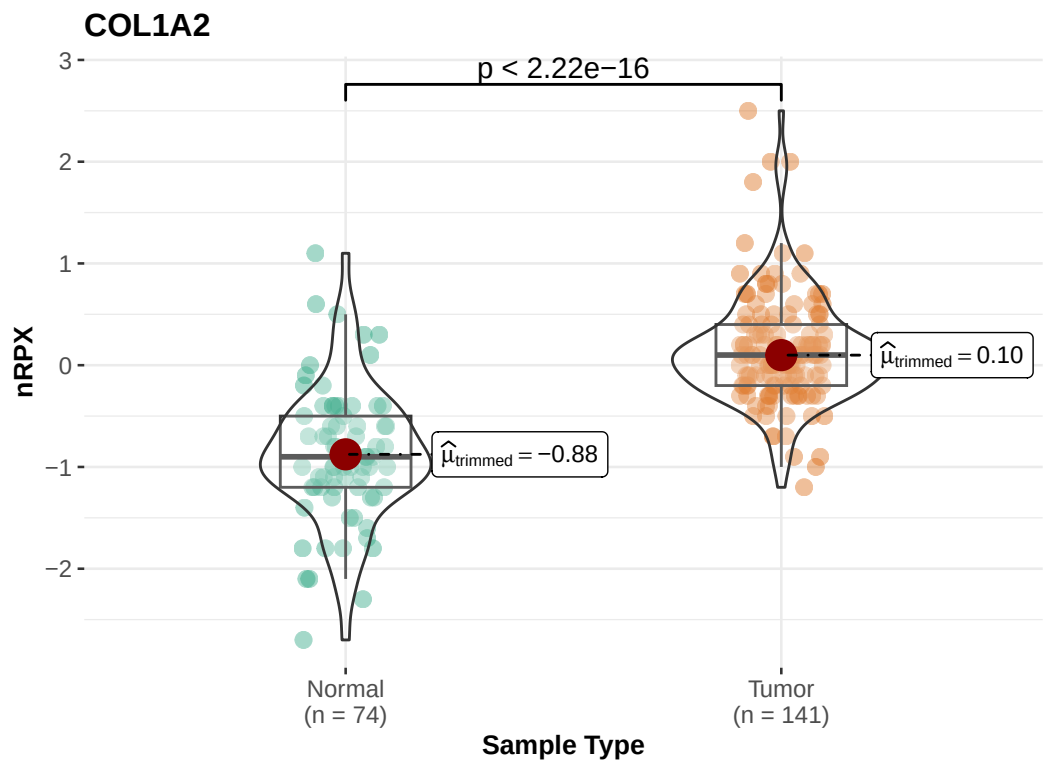


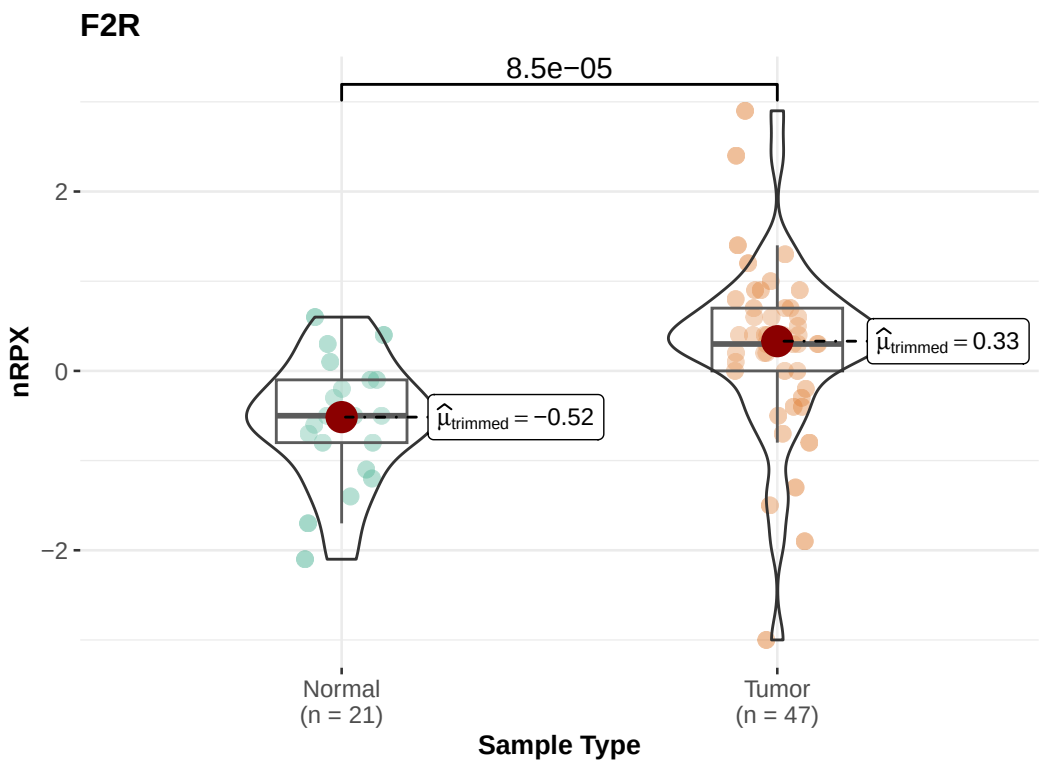
c

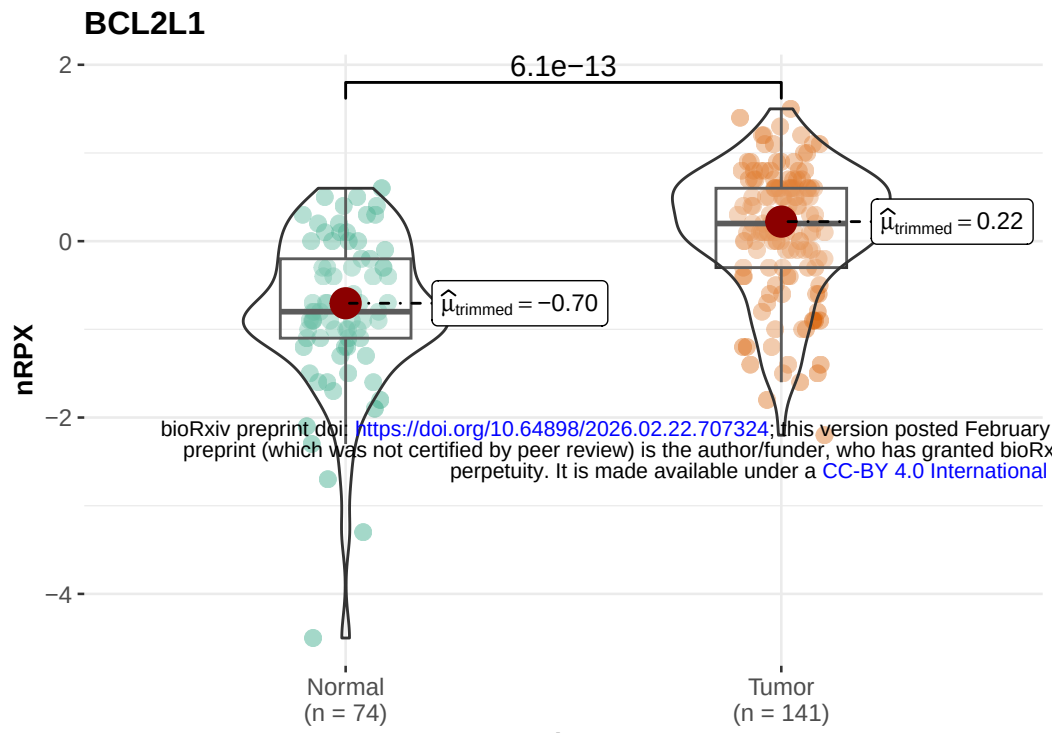


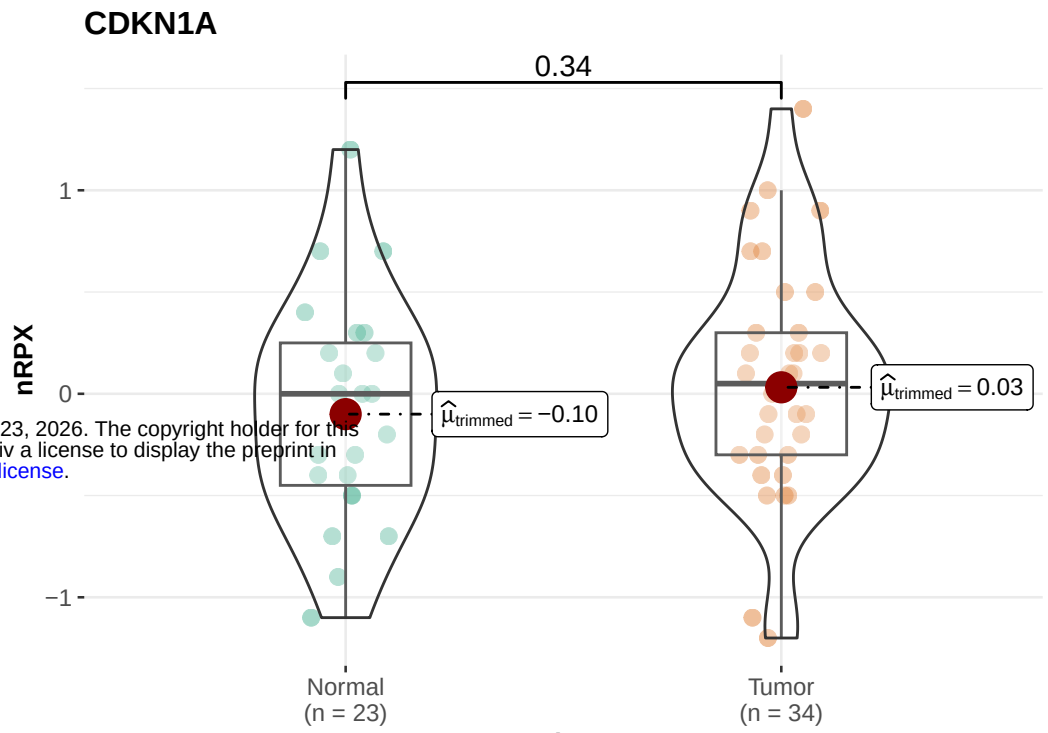
bioRxiv preprint doi: https://doi.org/10.64898/2026.02.22.707324; this version posted February 23, 2026. The copyright holder for this preprint (which was not certified by peer review) is the author/funder, who has granted bioRxiv a license to display the preprint in perpetuity. It is made available under a CC-BY 4.0 International license.



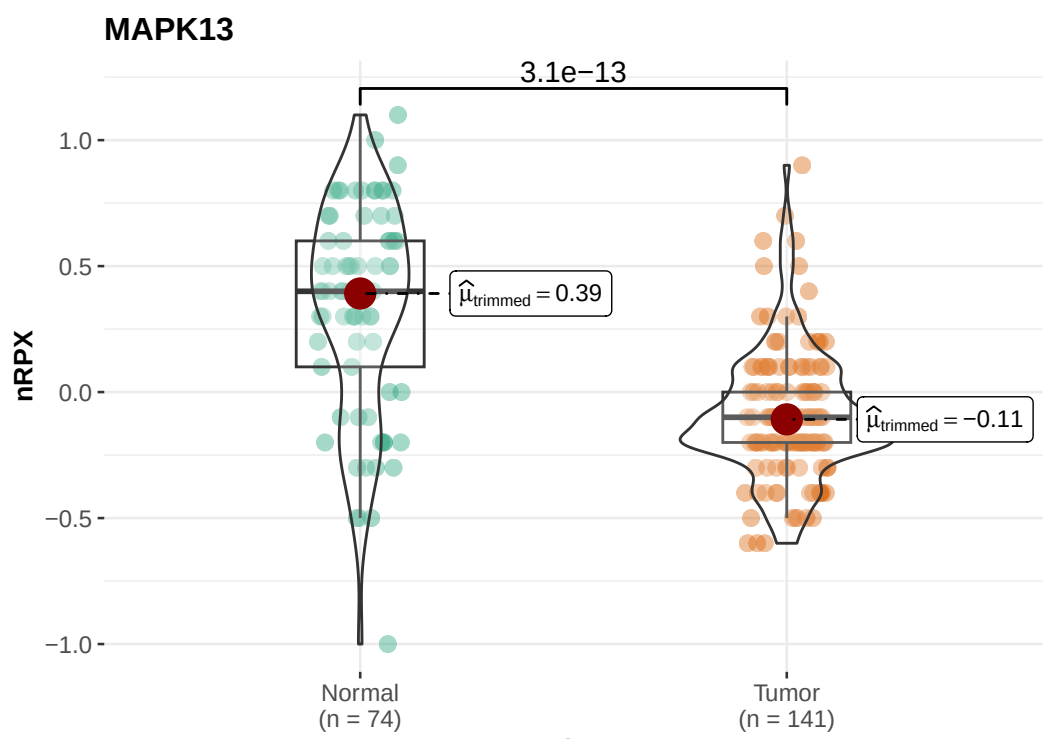


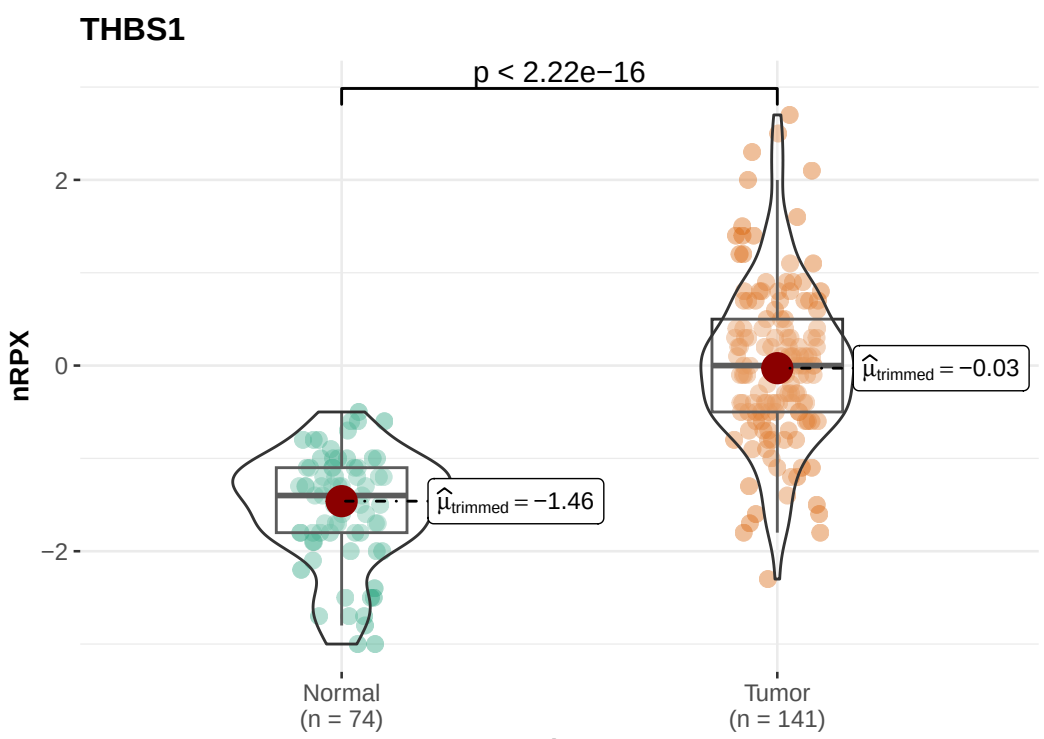


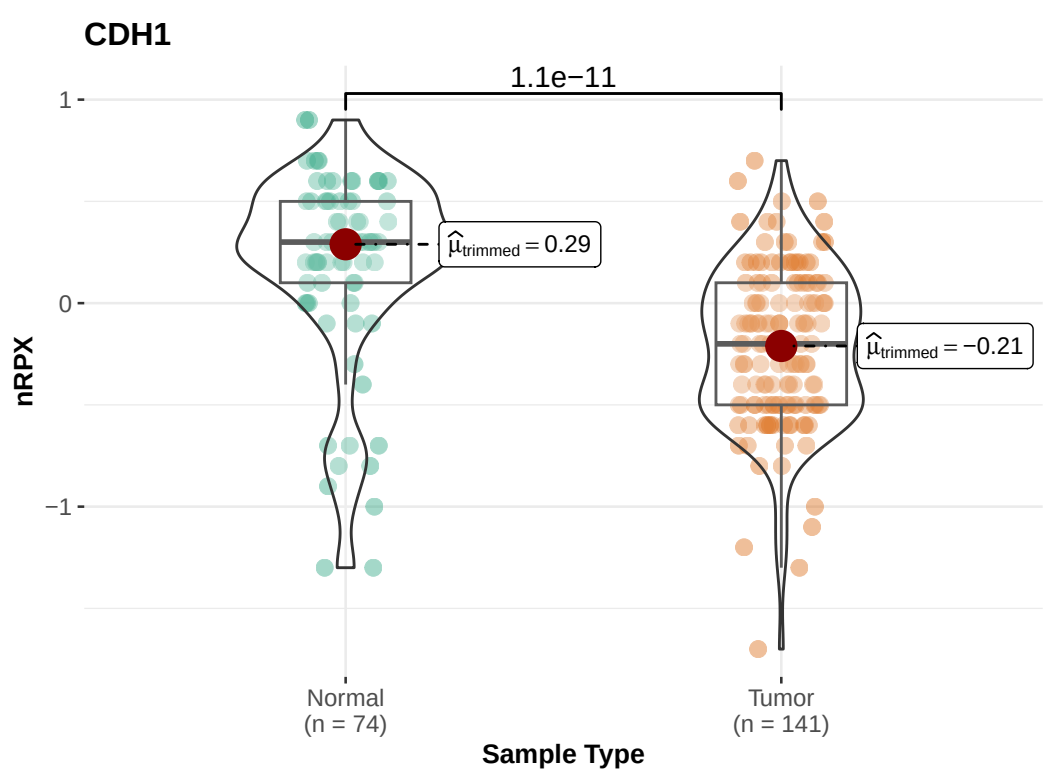


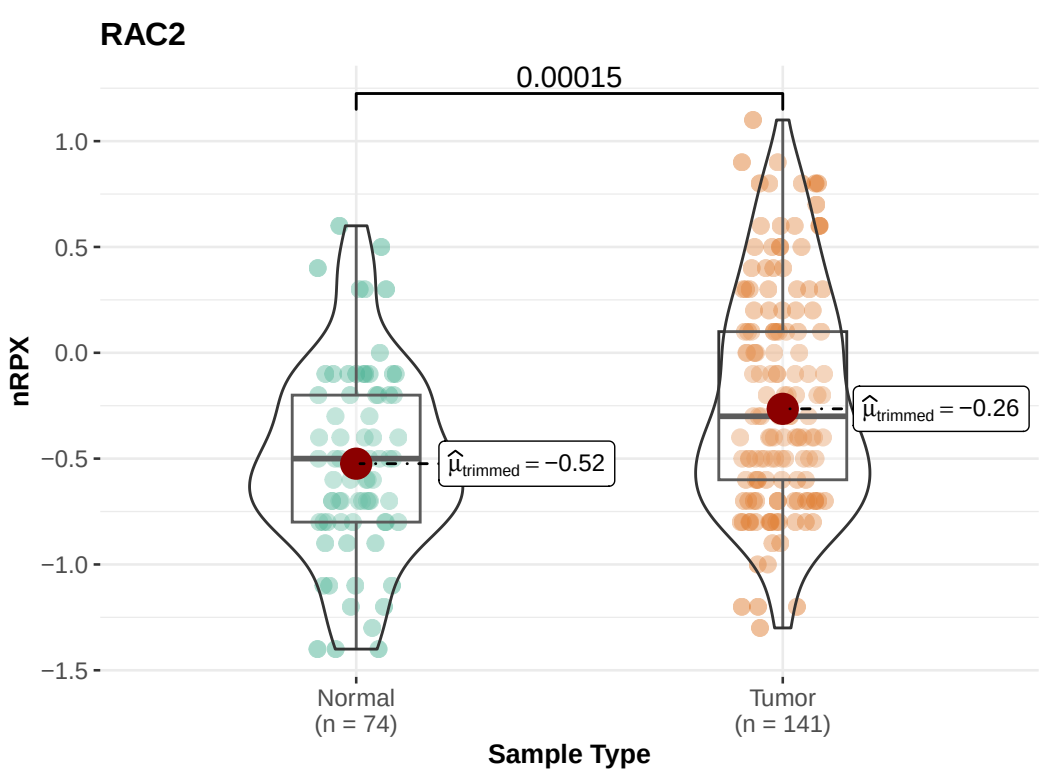


bioRxiv preprint doi: https://doi.org/10.64898/2026.02.22.707324; this version posted February 23, 2026. The copyright holder for this preprint (which was not certified by peer review) is the author/funder, who has granted bioRxiv a license to display the preprint in perpetuity. It is made available under a CC-BY 4.0 International license.

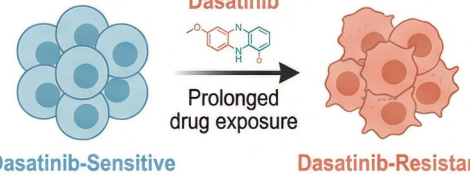


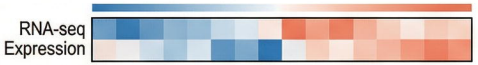






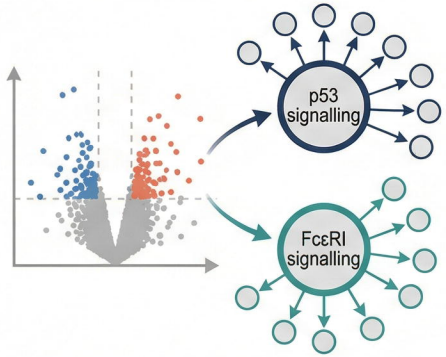
Drug Pressure & Experimental Context





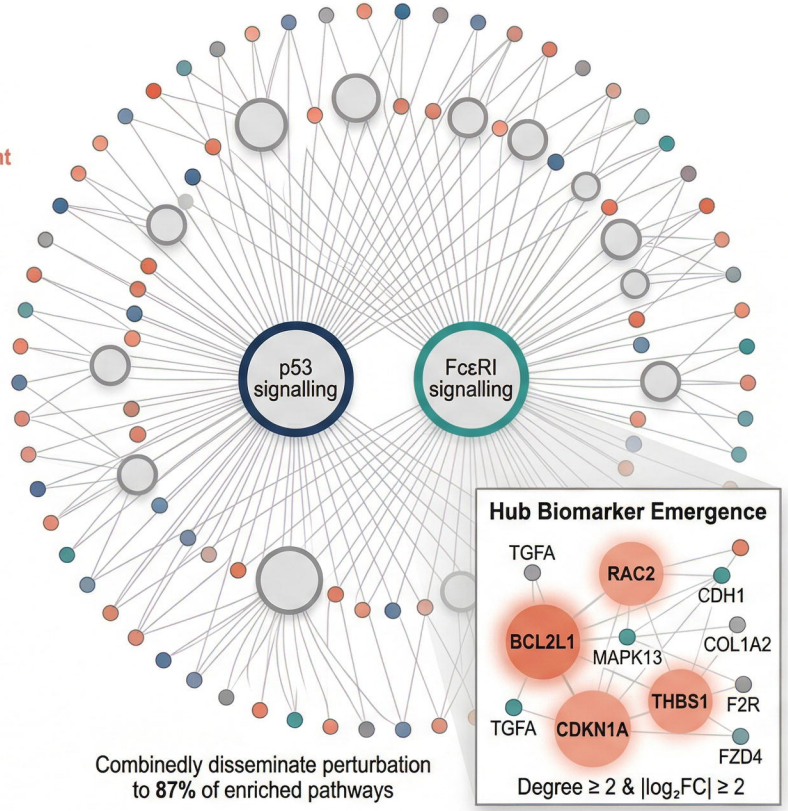
Transcriptomic profiling of resistant vs sensitive PDAC

Differential Expression & Pathway Enrichment



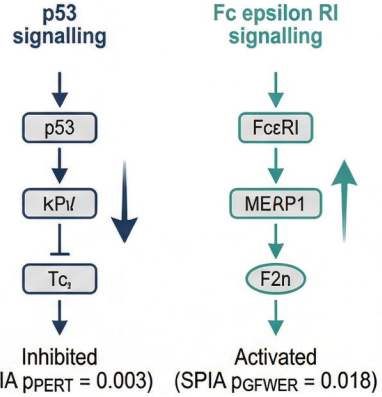
17 enriched KEGG signalling pathways

Cross-Talk Network

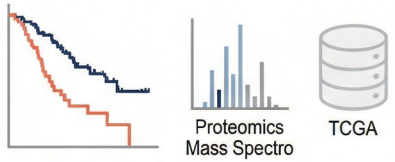


Combinedly disseminate perturbation to **87%** of enriched pathways

Pathway Impact & Functional Status



Clinical Validation



BCL2L1

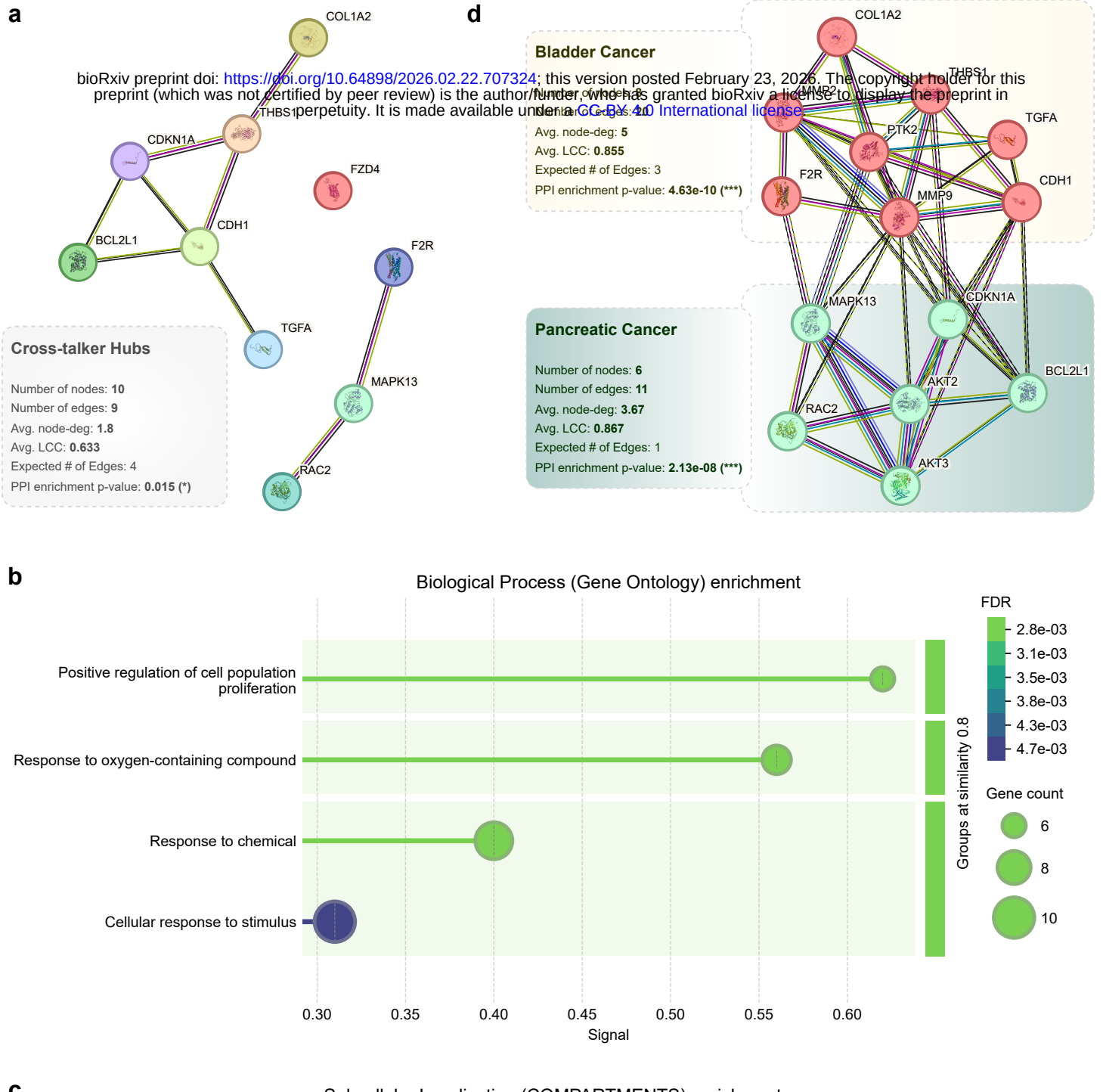
Pivotal global dissemination driver

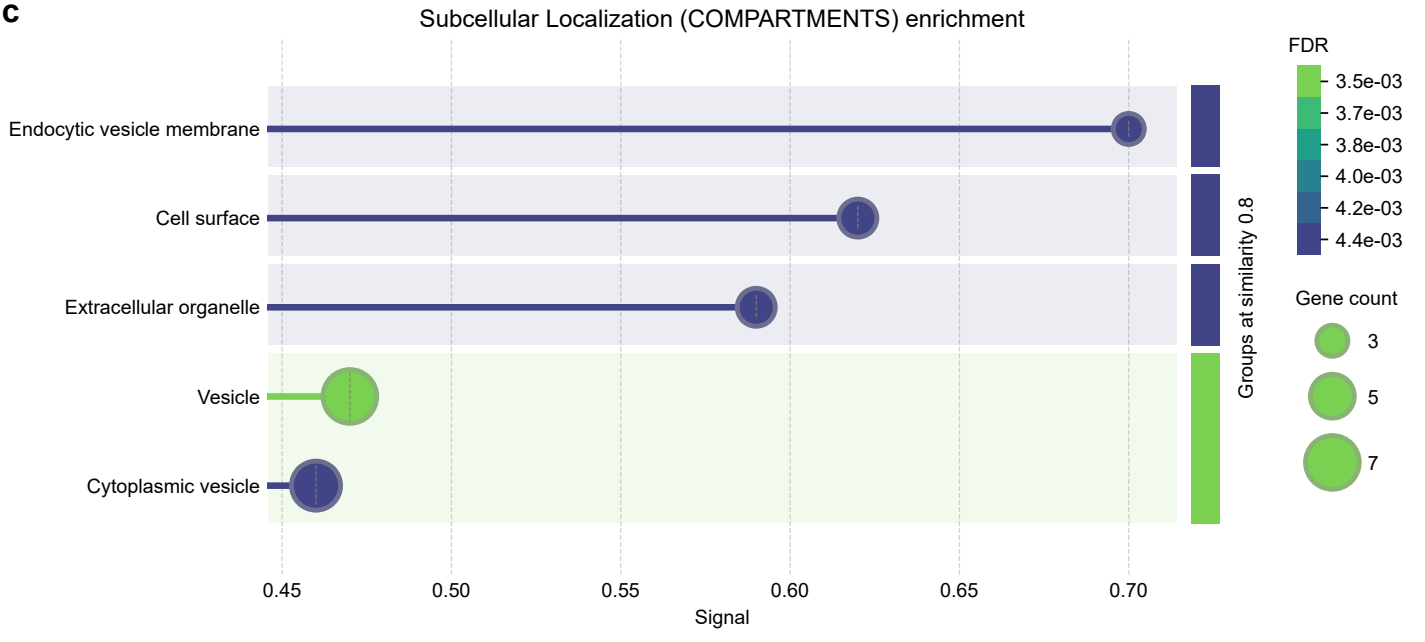
Prognostic in PAAD

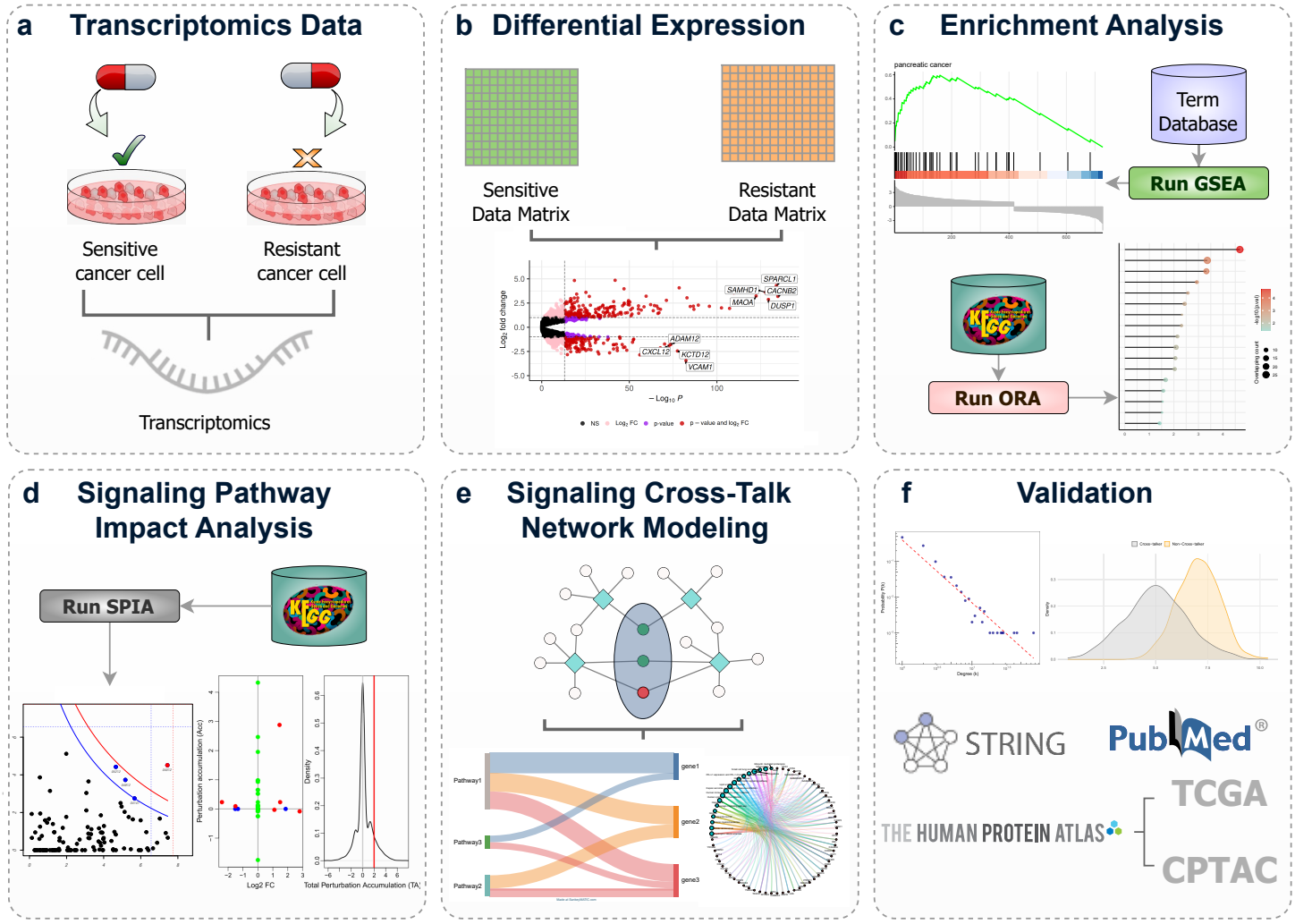
"Validated in TCGA & CPTAC datasets"

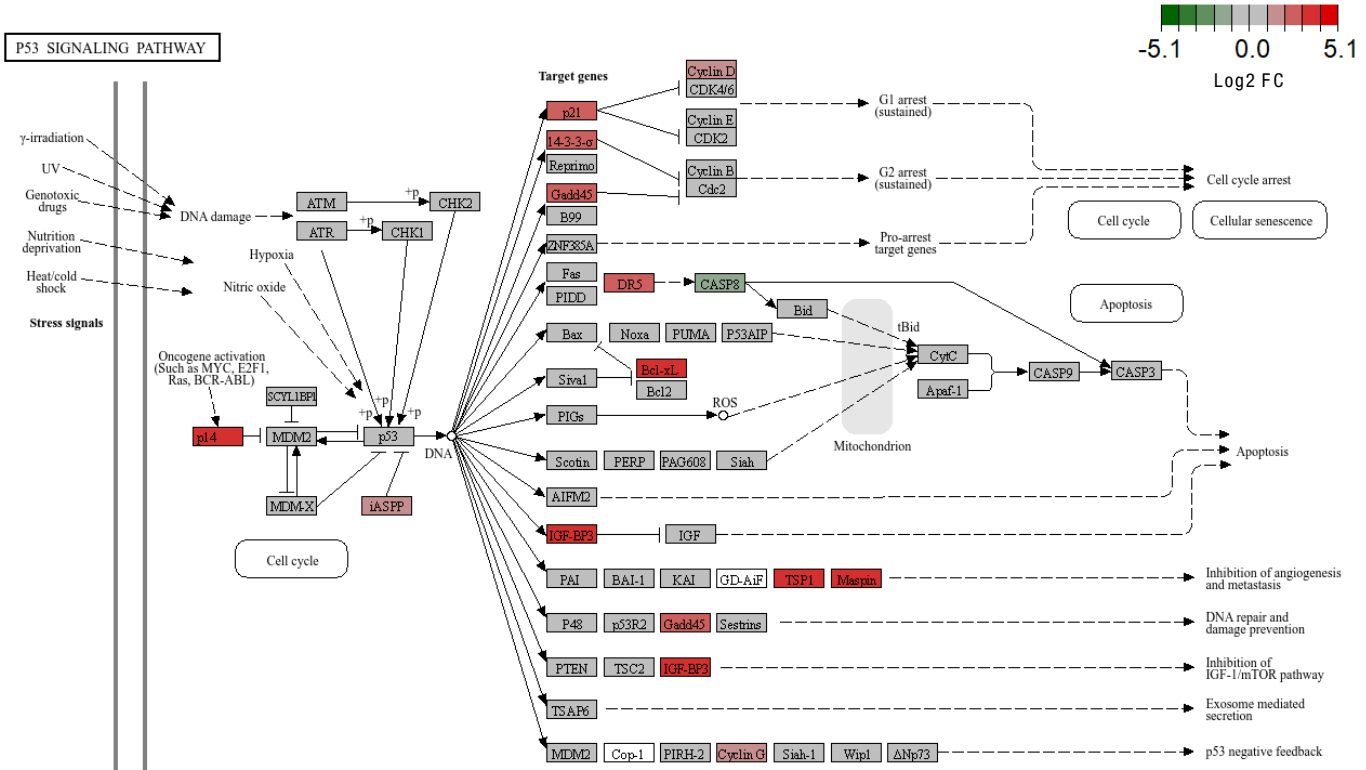
"Coordinated p53 suppression and FcεRI activation drive global signalling rewiring in acquired Dasatinib resistance."

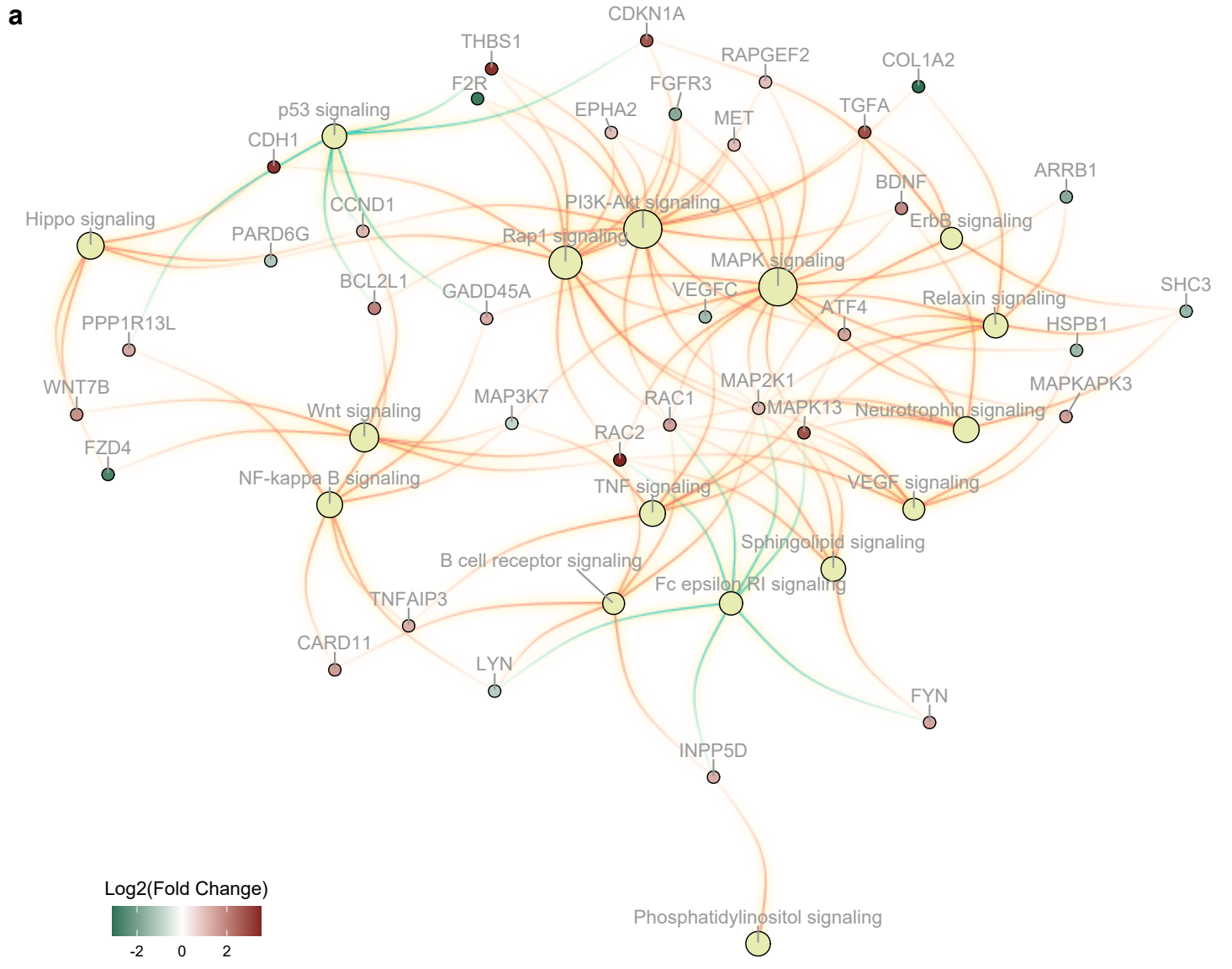
bioRxiv preprint doi: https://doi.org/10.64898/2026.02.22.707324; this version posted February 23, 2026. The copyright holder for this preprint (which was not certified by peer review) is the author/funder, who has granted bioRxiv a license to display the preprint in perpetuity. It is made available under a CC-BY 4.0 International license.

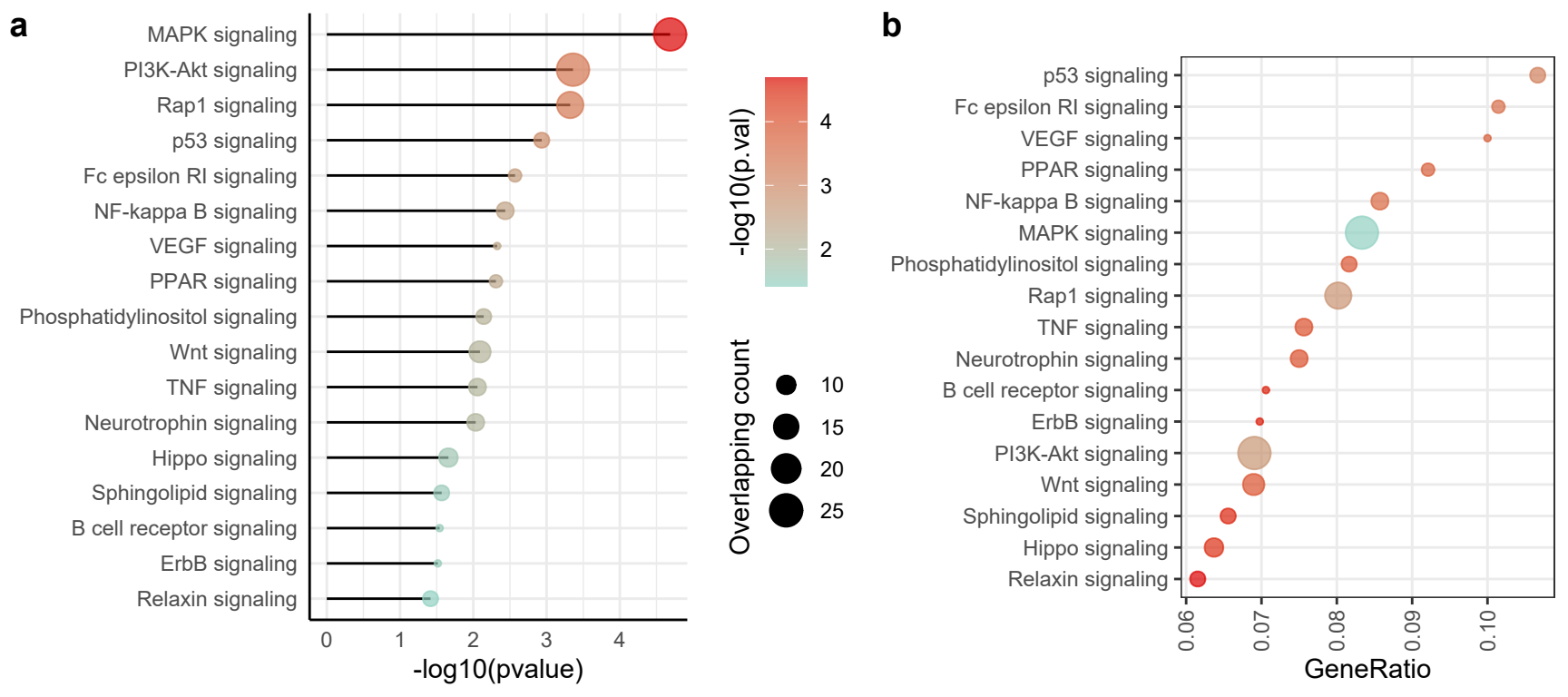


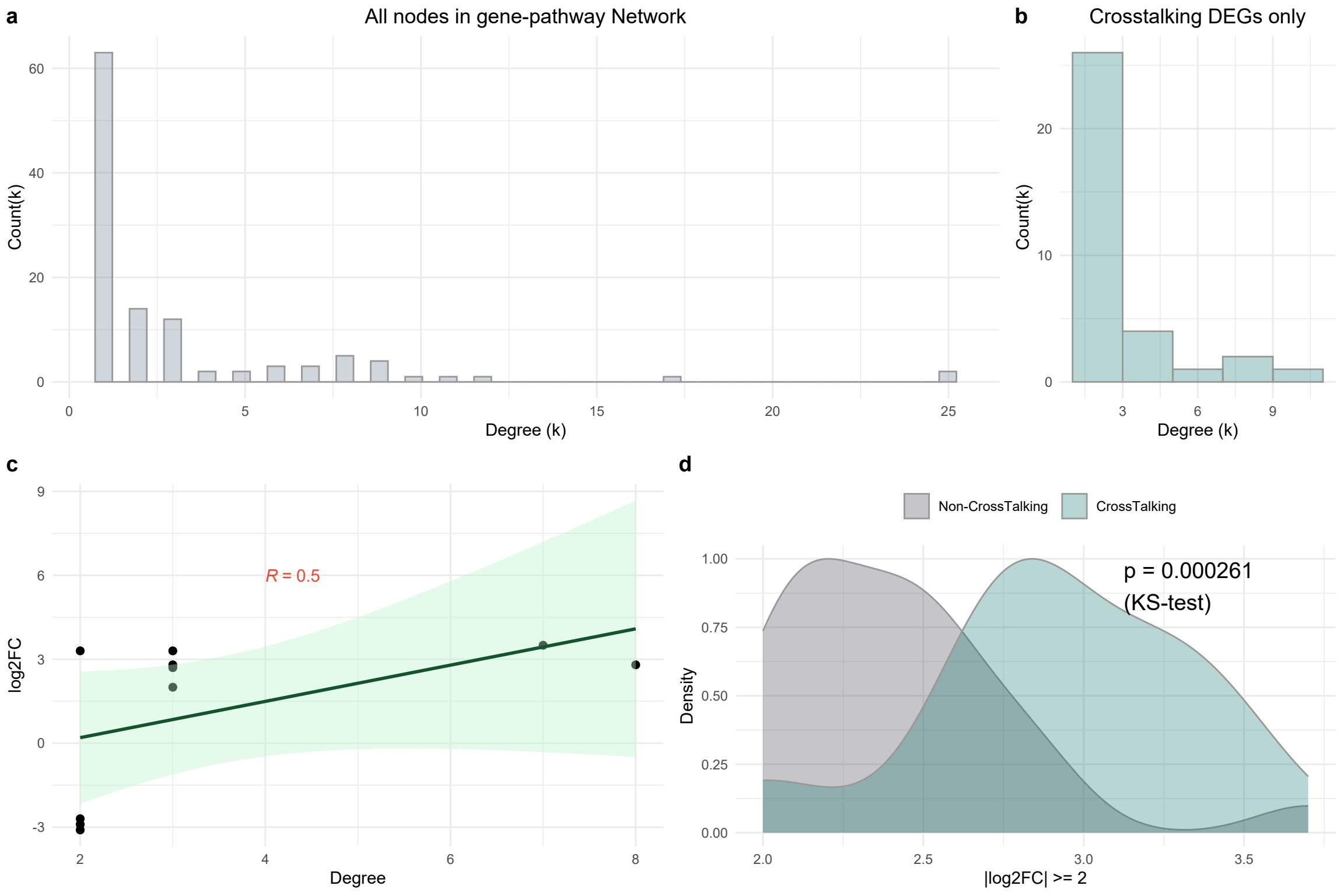


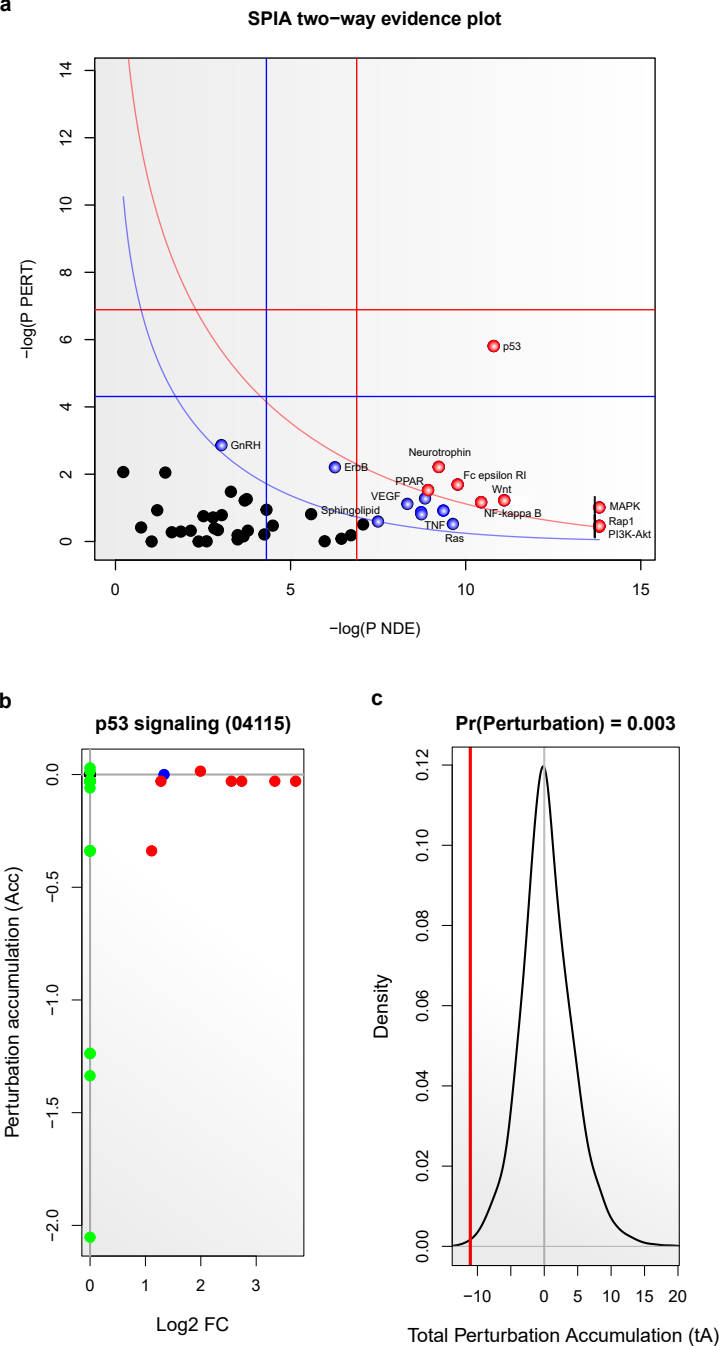

a Transcriptomics Data
Sensitive cancer cell
Resistant cancer cell
Transcriptomics
b Differential Expression
Sensitive Data Matrix
Resistant Data Matrix
SPARCL1
SAMHD1
CACNB2
MAOA
DUSP1
ADAM12
CXCL12
KCTD12
VCAM1
NS
p-value
c Enrichment Analysis
pancreatic cancer
Term Database
Run GSEA
Run ORA
d Signaling Pathway Impact Analysis
Run SPIA
Log2 FC
Total Perturbation Accumulation (TA)
e Signaling Cross-Talk Network Modeling
Pathway1
Pathway3
Pathway2
gene1
gene2
gene3
f Validation
STRING
PubMed
TCGA
THE HUMAN PROTEIN ATLAS
CPTAC

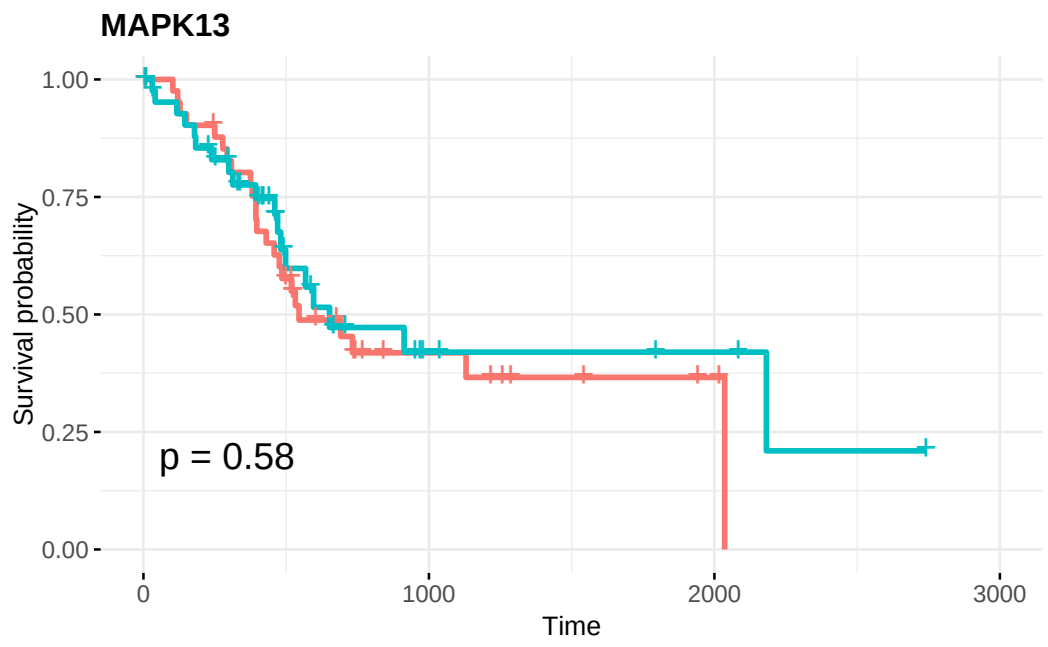

P53 SIGNALING PATHWAY
-5.1
0.0
5.1
Log2 FC
γ-irradiation
UV
Genotoxic drugs
Nutrition deprivation
Heat/cold shock
Stress signals
DNA damage
ATM
ATR
CHK2
CHK1
Hypoxia
Nitric oxide
Oncogene activation (Such as MYC, E2F1, Ras, BCR-ABL)
SCYL1BP1
p14
MDM2
MDM-X
p53
iASPP
DNA
Cell cycle
Target genes
p21
14-3-3-σ
Reprimo
Gadd45
B99
ZNF385A
Fas
PIDD
Bax
Noxa
PUMA
P53AIP
Siva1
Bcl-xL
Bcl2
PIGs
Scotin
PERP
PAG608
Siah
AIFM2
IGF-BP3
IGF
PAI
BAI-1
KAI
GD-AiF
TSP1
Maspin
P48
p53R2
Gadd45
Sestrins
PTEN
TSC2
IGF-BP3
TSAP6
MDM2
Cop-1
PIRH-2
Cyclin G
Siah-1
Wip1
ΔNp73
Cyclin D
CDK4/6
Cyclin E
CDK2
Cyclin B
Cdc2
G1 arrest (sustained)
G2 arrest (sustained)
Pro-arrest target genes
Cell cycle arrest
Cell cycle
Cellular senescence
DR5
CASP8
Bid
tBid
CytC
Apaf-1
CASP9
CASP3
Apoptosis
ROS
Mitochondrion
Apoptosis
Inhibition of angiogenesis and metastasis
DNA repair and damage prevention
Inhibition of IGF-1/mTOR pathway
Exosome mediated secretion
p53 negative feedback

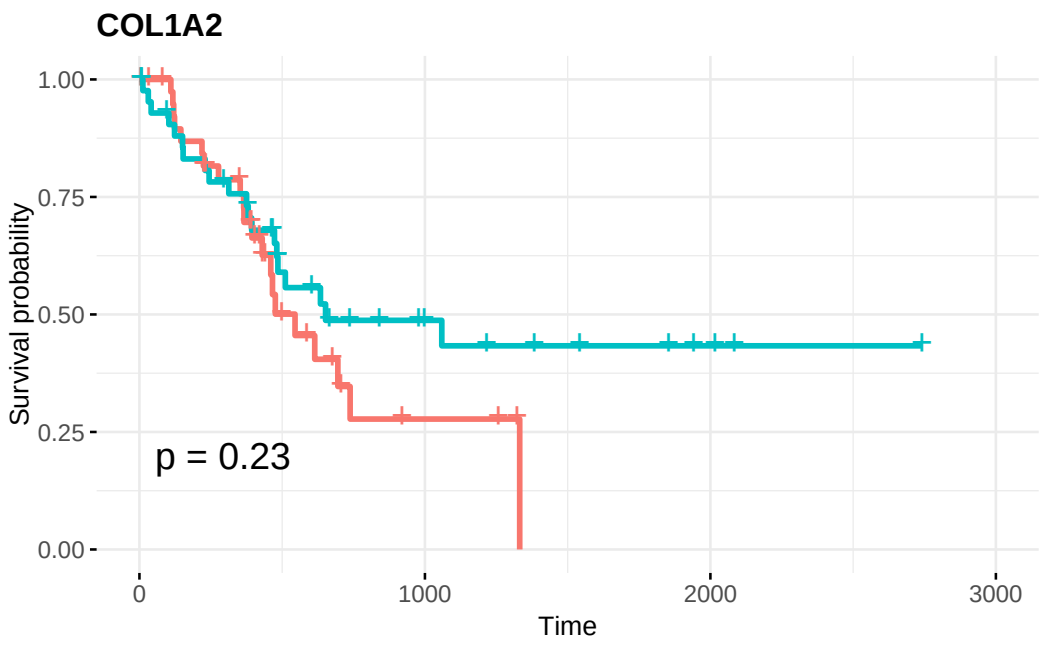

a
CDKN1A
THBS1
RAPGEF2
COL1A2
F2R
FGFR3
EPHA2
MET
TGFA
p53 signaling
CDH1
ARRB1
BDNF
CCND1
PI3K-Akt signaling
Hippo signaling
ErbB signaling
PARD6G
Rap1 signaling
MAPK signaling
BCL2L1
GADD45A
VEGFC
SHC3
ATF4
Relaxin signaling
PPP1R13L
HSPB1
MAP2K1
WNT7B
MAPKAPK3
MAP3K7
RAC1
MAPK13
Neurotrophin signaling
Wnt signaling
RAC2
FZD4
NF-kappa B signaling
TNF signaling
VEGF signaling
Sphingolipid signaling
B cell receptor signaling
Fc epsilon RI signaling
TNFAIP3
CARD11
LYN
FYN
INPP5D
Log2(Fold Change)
-2
0
2
Phosphatidylinositol signaling
b
All DEGs
727
Cross-talker DEGs
34
p53 Signalling
6
Cross-talker Hubs
10
FC epsilon RI Signalling
7
Distribution of DEGs in Dastatinib Resistance
17
All Enriched Signaling Pathway
16
Cross-talking Pathways Only
87%
With FC epsilon RI Signalling
7
6
13
With p53 Signalling
Distribution of Enriched Signaling pathways in Dastatinib Resistance

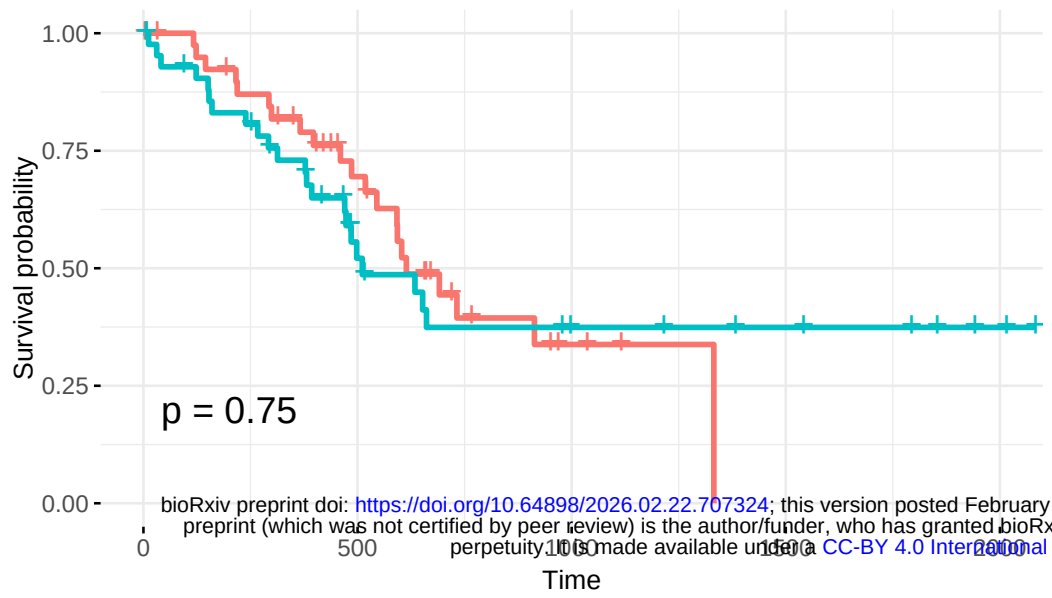

a
MAPK signaling
PI3K-Akt signaling
Rap1 signaling
p53 signaling
Fc epsilon RI signaling
NF-kappa B signaling
VEGF signaling
PPAR signaling
Phosphatidylinositol signaling
Wnt signaling
TNF signaling
Neurotrophin signaling
Hippo signaling
Sphingolipid signaling
B cell receptor signaling
ErbB signaling
Relaxin signaling
0
1
2
3
4
-log10(pvalue)
-log10(p.val)
4
3
2
Overlapping count
10
15
20
25
b
p53 signaling
Fc epsilon RI signaling
VEGF signaling
PPAR signaling
NF-kappa B signaling
MAPK signaling
Phosphatidylinositol signaling
Rap1 signaling
TNF signaling
Neurotrophin signaling
B cell receptor signaling
ErbB signaling
PI3K-Akt signaling
Wnt signaling
Sphingolipid signaling
Hippo signaling
Relaxin signaling
0.06
0.07
0.08
0.09
0.10
GeneRatio

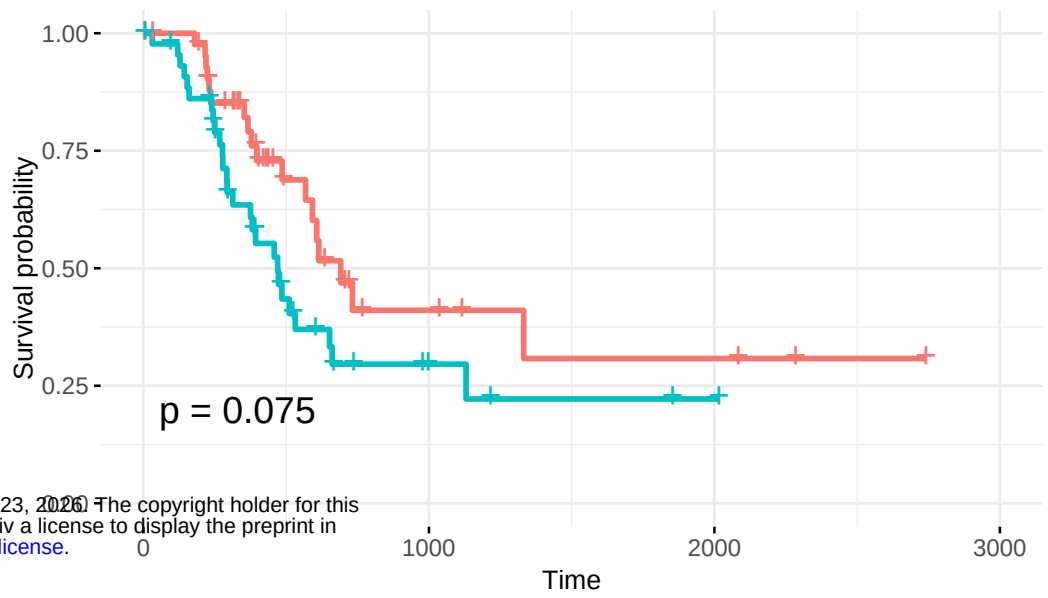

a
All nodes in gene-pathway Network
Count(k)
Degree (k)
b
Crosstalking DEGs only
Count(k)
Degree (k)
c
R = 0.5
log2FC
Degree
d
Non-CrossTalking
CrossTalking
p = 0.000261
(KS-test)
Density
|log2FC| >= 2


a
SPIA two−way evidence plot
−log(P PERT)
−log(P NDE)
p53
GnRH
ErbB
Neurotrophin
Fc epsilon RI
PPAR
Wnt
VEGF
NF−kappa B
Sphingolipid
TNF
Ras
MAPK
Rap1
PI3K−Akt
b
p53 signaling (04115)
Perturbation accumulation (Acc)
Log2 FC
c
Pr(Perturbation) = 0.003
Density
Total Perturbation Accumulation (tA)









bioRxiv preprint doi: https://doi.org/10.64898/2026.02.22.707324; this version posted February 23, 2026. The copyright holder for this preprint (which was not certified by peer review) is the author/funder, who has granted bioRxiv a license to display the preprint in perpetuity. It is made available under a CC-BY 4.0 International license.

